

Mapping a Biogenetic Oxidation-Reduction Plume Using
Spontaneous Potential at a Field Site in Oyster, Virginia

A Thesis
Submitted to
The Temple University Graduate Board

In Partial Fulfillment
Of the Requirements for the Degree
MASTER OF ARTS

by
Gregory James Korniewicz
January, 2000

Jonathan Nyquist, Thesis Advisor

Laura Toran, Committee Member

Peter Goodwin, Committee Member

ABSTRACT

At a contaminated site near Oyster Virginia, spontaneous potential (SP) measurements correlate closely with dissolved oxygen (DO) data from wells, indicating that a contaminant plume can be identified by this geophysical method. The field site is a 200 m X 190 m grassy field underlain by electrically homogeneous, Pleistocene, semi-consolidated sands bearing oxidized groundwater. At this site, DO measurements from 28 wells revealed a zone of reduction created by the biodegradation of buried tomato waste leaching from trenches. SP was measured using two sampling techniques: along a grid of 16 transects at 3 m intervals; and at 5 m intervals along 7 selectively oriented transects between significant wells. Spatial distribution of SP values compared favorably with the patterns formed by the DO data. This correlation was confirmed by the non-parametric Spearman rank correlation analysis, along two transects perpendicular to the redox boundary, which revealed a strong negative correlation between DO and SP at the 99% confidence level. Other potential sources of SP were ruled out by the use of resistivity, magnetometry, and ground penetrating radar,

thus isolating redox potentials as the sole cause of SP.
Therefore, SP can be used to map zones of reduction present
in oxidized subsurfaces when all other sources of SP can be
eliminated.

ACKNOWLEDGEMENTS

I would foremost like to thank Peter Goodwin, Jon Nyquist, Laura Toran, David Grandstaff and the rest of the faculty and staff at Temple University; without their help this thesis would have never been possible. I would also like to thank the following people for helping me achieve my academic successes: Mom, Dad, Shell, Joey, and Grandma K.; Jeff Over, Richard Young, Mayor Hathaway, and the rest of the faculty and staff at Geneseo; Aaron Mills, Amy Callaghan, Chuck Fleer, and the rest of the LTER staff; the Geneseo Funk Mob. Thank you all very much.

TABLE OF CONTENTS

	Page
ABSTRACT	ii
ACKNOWLEDGEMENTS	iv
LIST OF TABLES	viii
LIST OF FIGURES	ix
CHAPTER	
1. INTRODUCTION	1
A. Spontaneous Potential Background	1
B. SP and Redox Potentials	5
C. Thesis Hypothesis and Objectives	10
2. SITE OVERVIEW	12
A. Site Location	12
B. Site History	12
C. Stratigraphy	15
D. Previous Studies	19
E. Preliminary SP Survey	22
3. MEASUREMENT OF REDOX CONDITIONS	25
A. Objectives	25
B. Methods	25

C. Results	30
4. BACKGROUND GEOPHYSICAL SURVEYING	32
A. Objectives	32
B. The Survey Grid	32
C. Magnetic Survey	33
i. Objectives	33
ii. Methods	33
iii. Results	37
D. Resistivity	37
i. Objectives	37
ii. Methods	39
iii. Results	40
E. Ground Penetrating Radar	46
i. Objectives	46
ii. Methods	46
iii. Results	48
F. Conclusions from Geophysical Surveying	51
5. SPONTANEOUS POTENTIAL	52
A. Objectives	52
B. Methods	52
C. Results	54

6. CONCLUSIONS	61
A. Summary and Implications	61
B. Suggestions for Future Work	63
REFERENCES CITED	65

LIST OF TABLES

Table 2-1. Summarized Biogeochemical Data.	21
Table 3-1. Eh Measurements from Wells	25
Table 4-1. Magnetic Susceptibilities of Various Materials	34

LIST OF FIGURES

Figure 1-1.	A Typical SP Setup	2
Figure 1-2.	A Voltaic Cell	6
Figure 1-3.	Sato and Mooney's (1960) Model for how Sulfide Deposits Create Redox Potentials	8
Figure 1-4.	Corry's (1985) Model for how Sulfide Deposits Create Redox Potentials	9
Figure 2-1.	Location of the Oyster, VA Field Site	13
Figure 2-2.	Geologic Map and Cross-Section of the Delmarva Peninsula	16
Figure 2-3.	Exposure of the Nassawadox/Wachapreague Contact at Kiptopeke State Park	18
Figure 2-4.	Geology of the Field Site	20
Figure 2-5.	Results of the Preliminary SP Survey	23
Figure 3-1.	Equipment Setup for Collecting DO Data	28
Figure 3-2.	DO Measurements Made Using a CHEMET™	29
Figure 3-3.	Contoured DO and Head Levels	31
Figure 4-1.	Magnetic Nonogram for Estimating Anomaly Magnitude	36
Figure 4-2.	Vertical Magnetic Gradient Surface Map	38
Figure 4-3.	Location of Resistivity Survey Lines	41
Figure 4-4.	2D-Resistivity Cross-Section Along Line 1 ...	42
Figure 4-5.	2D-Resistivity Cross-Section Along Line 2 ...	43
Figure 4-6.	2D-Resistivity Cross-Section Along Line 3 ...	44

Figure 4-7.	Results from the 100 MHz GPR Survey Along the Southern Road	49
Figure 4-8.	Results from the 250 MHz GPR Survey of the Nassawadox Formation Parallel to Strike	50
Figure 5-1.	Contour Map of DO and SP1	55
Figure 5-2.	Contour Map of DO and SP2	56
Figure 5-3.	Plot of DO and SP Versus Distance for W2-AC1 and A3-TS5	58
Figure 5-4.	Plot of DO Versus SP for W2-AC1 and A3-TS5 ..	59

CHAPTER 1

INTRODUCTION

A. Spontaneous Potential Background

SP is the geophysical technique of measuring naturally occurring voltage potentials in the subsurface. SP measurements are made by recording the voltage potential between two non-polarizing electrodes inserted in the ground (Figure 1-1).

Spontaneous Potential (SP) is one of the oldest known geophysical methods. Robert Fox in Cornwall, England developed it back in 1830 to find underground copper sulfide deposits, which is still the number one use of SP today (Reynolds, 1997). Instead of identifying the location of a sulfide deposit, I used SP to locate a plume of reduced groundwater. To test the correlation between oxidation-reduction (redox) potentials and SP, I needed to map SP over an area containing oxidizing and reducing zones; each zone should have characteristic SP values.

There are many sources of voltage potentials, natural and man-made (Ernstson and Scherer, 1986; Corwin, 1991; Reynolds, 1997). For example, the movement of water through a porous medium generates a streaming potential.

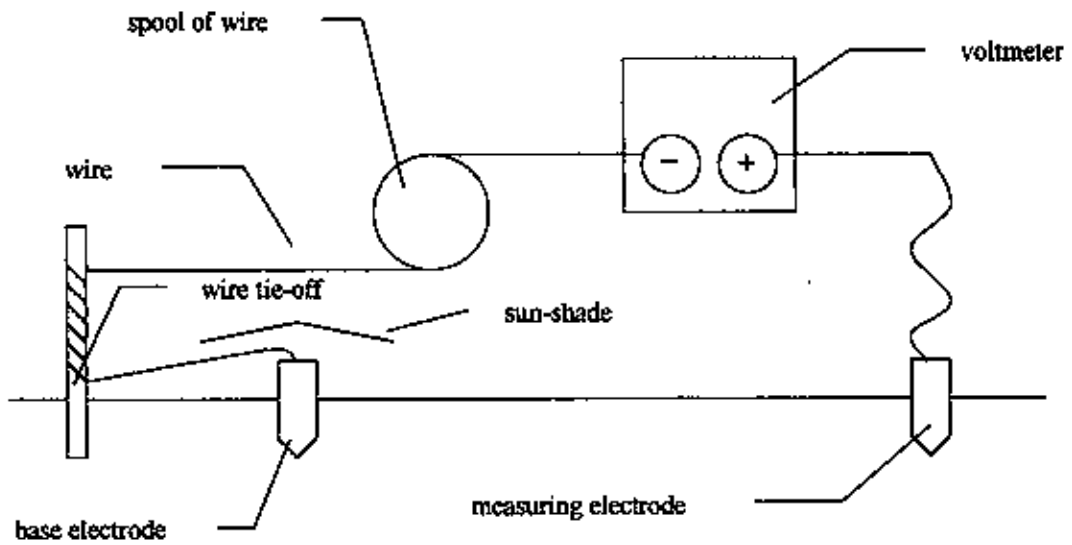


Figure 1-1. A Typical SP Setup. An electrical potential is measured between the base electrode and the measuring (roving) electrode using a spool of wire and a voltmeter. To prevent pulling the wire off of the base electrode, a wire tie-off is used. The negative and positive leads attach to the base electrode and roving electrode, respectively. A sun-shade covers the base electrode to avoid voltages associated with temperature differences between the electrodes (from Corwin, 1984).

The magnitude of the streaming potential is defined by equation (1-1) for the electrokinetic potential (E_k):

$$E_k = \frac{\epsilon \mu C_E \delta P}{4\pi \eta} \quad (1-1)$$

Symbols ϵ , μ and η are the dielectric coefficient, resistivity, and dynamic viscosity of the electrolyte, respectively. The change in pressure is δP . The ease with which cations are stripped from their host rock is determined by the coupling coefficient, C_E . Subsurface structures such as faults, stratigraphic boundaries, and fracture zones create areas of preferential flow that can lead to elevated potentials. Increased precipitation can also elevate these values.

Streaming potentials arising from pressure gradients controlled by topography are called topographic potentials. Topographic potentials increase with progressively steeper gradients. Topographic effects can be very large (-2,693 mV on the peak of Hoover Volcano in Alaska), but can be ignored if the topographic gradient is less than 20 degrees (Ernstson, 1986).

An electrochemical potential is generated by a concentration gradient between two formations. The size of this potential is defined by equation (1-2) for the Nernst potential (E_N):

$$E_N = -\frac{RT}{nF} \ln(C_1/C_2) \quad (1-2)$$

Symbols R, T, n, and F are the universal gas constant, temperature, ionic valence, and Faraday's constant, respectively. The solution concentrations of the pore waters are C_1 and C_2 . For example, a cation ratio of 5:1, for NaCl, between two formations, leads to a 50 mV SP anomaly (Reynolds, 1997).

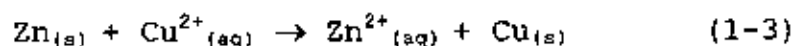
Thermoelectric potentials are created by high temperature gradients. The causes of thermoelectric potentials have not been extensively studied and are poorly understood (Telford et al., 1990). Changes in groundwater temperature can be due to rainfall, volcanic activity or buried man-made items such as generators. Finally, cathodically protected pipes, power lines, corrosion of buried metal and transmission towers are all examples of man-made electrical noise that can affect SP.

Since SP arises from a multitude of sources, SP data are often difficult to interpret. Despite these

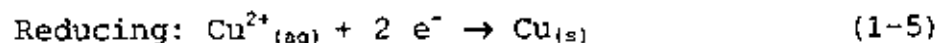
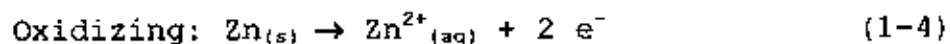
difficulties of interpretation, SP is commonly used because data are easily and affordably collected.

B. SP and Redox Potentials

Redox potentials are electrochemical potentials associated with a spontaneous reaction between a reducing agent and an oxidizing agent (Chang, 1996). The basic principle behind a voltaic cell is to separate the redox reaction into two half-cells connected by electrical and ionic pathways. For example, the redox reaction between solid zinc and aqueous copper (Figure 1-2) can be expressed as the chemical reaction in equation 1-3:



This chemical reaction can be broken down into two half-reactions, one oxidizing and one reducing as expressed in equations 1-4 and 1-5:



The zinc strip ($\text{Zn}_{(s)}$) is immersed in a zinc sulfate solution, forming one of the half-cells. The zinc is oxidized to its aqueous form and gives off two electrons. These electrons travel through the wire and reduce the $\text{Cu}^{2+}_{(aq)}$ in the cuprous sulfate solution present in the

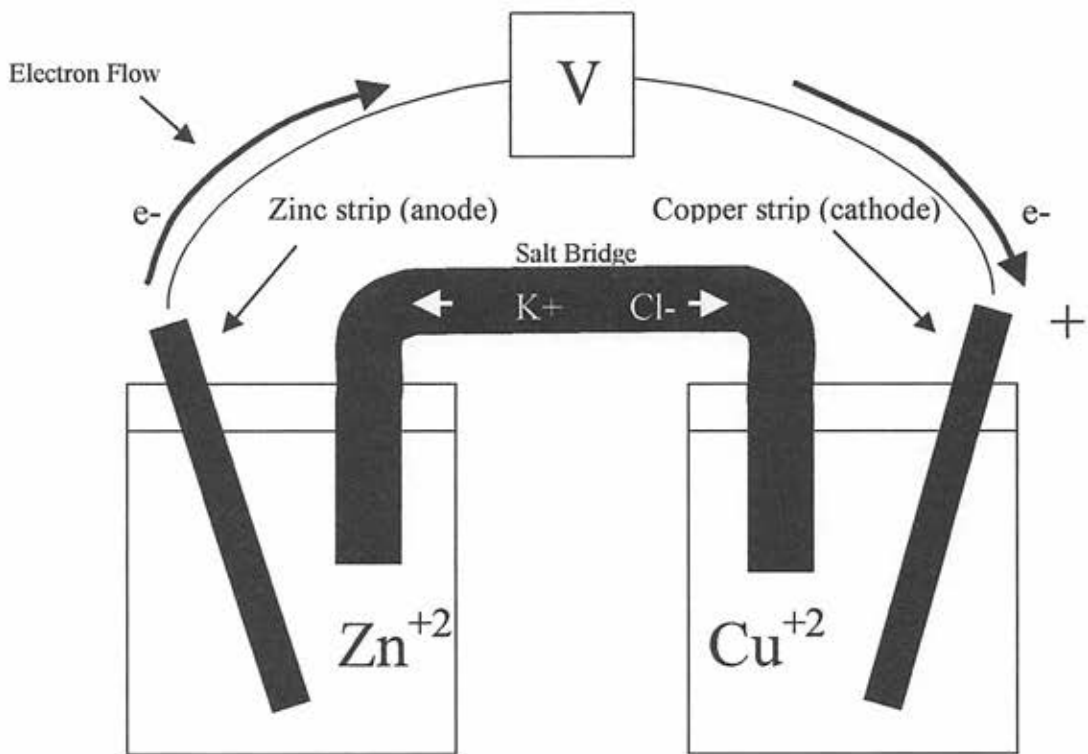


Figure 1-2. A Voltaic Cell. A voltaic cell harnesses the electrical work of a spontaneous chemical reaction. The voltmeter (V) measures the potential between the two cells. The zinc and copper strips act as electrodes and the salt bridge (a potassium chloride solution) allows ions to flow between the beakers without allowing the solutions to mix. When the circuit joining the two systems is completed, the reaction generates an electric current.

other half-cell to form $\text{Cu}_{(s)}$. Ions move through the salt bridge to maintain the charge balance of the two solutions.

Sato and Mooney (1960) gave the classical explanation of how redox reactions, associated with sulfide deposits, generate an SP anomaly (Figure 1-3). Two half-cells are created when the groundwater table intersects a sulfide deposit. Reduction reactions occur in the lower half-cell, while oxidation reactions occur in the upper half-cell. Electrons flow between the two zones through the conductive ore body; transfer of cations occurs in the surrounding medium.

Corry (1985) presented a competing theory on how redox potentials are created by sulfide ore deposits. Corry argued that Sato and Mooney's model could not explain SP anomalies measured over a sulfide deposit that is located completely above or below the water table. Corry also pointed out that in Sato and Mooney's model, sulfide deposits are continually discharging; yet SP anomalies over sulfide deposits remain stable for decades.

Corry proposed that redox potentials exist between sulfide deposits and the surrounding medium (Figure 1-4). This electrochemical potential generates electrical current only when SP instrumentation provides an electrical pathway

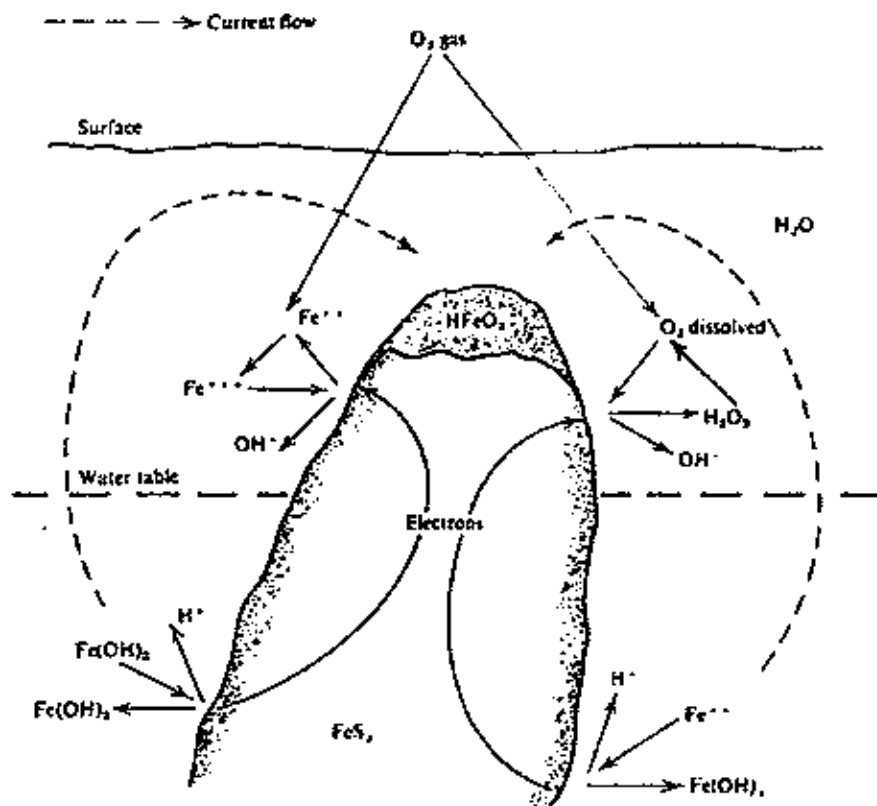


Figure 1-3. Sato and Mooney's (1960) Model for how Sulfide Deposits Create Redox Potentials. Two half-cells are created when the groundwater table intersects a sulfide deposit. Reduction reactions occur in the lower half-cell, while oxidizing reactions occur in the upper half-cell. Electrons flow between the two zones through the conductive ore body; transfer of cations occurs in the surrounding medium.

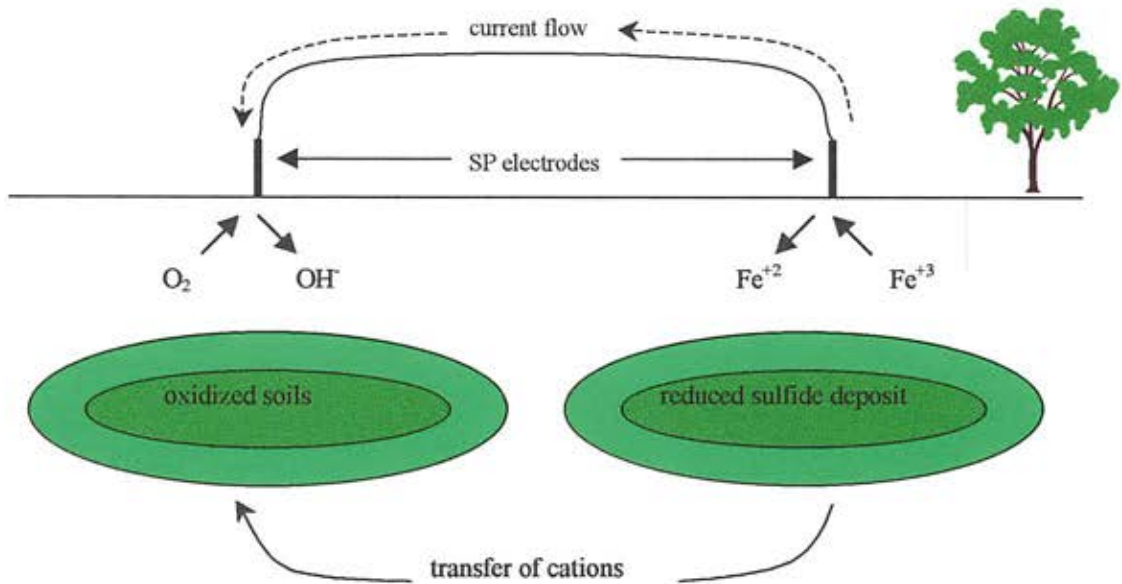


Figure 1-4. Corry's (1985) Model for how Sulfide Deposits Create Redox Potentials. The two half-cells are the reduced sulfide deposit and the oxidized background medium. Electrons flow from the reduced zone to the oxidized zone. The background medium serves as a salt bridge allowing ionic flow between the two zones. An electrochemical voltage potential is measured between the two SP electrodes.

for electrons between the two zones. The surrounding medium acts like a salt bridge, providing a pathway for cations between the two zones. The sulfide represents a reducing environment while the background medium is an oxidizing one. These are the two half-cells of the system. Voltage potentials between the oxidizing and reducing environments would be greater than voltage potentials between two electrodes present solely in one of the zones, where voltage potential is theoretically zero. Corry's (1985) model is not limited to sulfides; in theory any neighboring zone of reduction and oxidation should produce SP anomalies.

C. Thesis Hypothesis and Objectives

I conducted a study at a field site in Oyster, Virginia to see whether Corry's (1985) model for SP anomalies could explain the electrical potential between a plume of reduced groundwater and an oxidizing background medium. I correlated SP with redox by comparing the distribution of SP values to the distribution of redox values in a field area with a biogenetic plume of reduced groundwater.

Demonstrating the correlation between SP and redox conditions depended on showing that the redox potentials associated with a plume of reduced groundwater were the

sole cause of the SP anomalies. Other (non-redox) SP sources were systematically examined and dismissed through the use of mineralogical and geophysical evidence. The use of SP for identifying zones of reduced organic contaminants has been hypothesized (Corry et al., 1996), but never thoroughly studied.

Using SP to map redox conditions could be developed into a technique for monitoring contaminant spills, and would provide a cost-effective way of monitoring bioremediation. In recent years, bioremediation has proven to be a viable alternative to traditional remediation methods, such as pump and treat, because of its affordability and effectiveness. Taking groundwater samples from wells is the most popular method to date for mapping the extent and shape of a contaminant plume being biodegraded. The collection of groundwater samples is costly and time consuming. The development of SP as a method for mapping redox zones could provide a quick, cheap and accurate way to monitor the bioremediation of an organic contaminant.

CHAPTER 2

SITE OVERVIEW

The study area is located at N 38° 17' 43", W 75° 55' 20", 15 miles north of the southern tip of the Delmarva Peninsula, outside the small fishing town of Oyster, Va. It is part of an area managed by the Virginia Coast Reserve/Long-Term Ecological Research Project (VCR/LTER), which has been funded by the National Science Foundation (NSF) for 14 years. The study area is a small, coastal, farm field across the street from the LTER field house (Figure 2-1).

B. Site History

The northwest portion of the study area was used for the dumping of tomato cannery waste in the late 1970's. Tomato waste (e.g. rotten tomatoes, skins, seeds) was thrown into trenches dug at the field site and covered with sand removed from the trenches (Knapp and Thompson, 1998).

The northwestern portion of the field area contains five trenches, covering an area approximately 100 m long and 75 m wide. The trenches appear as 1 m-deep depressions that formed by the decay tomato waste leading to subsidence of the ground surface.



(a)

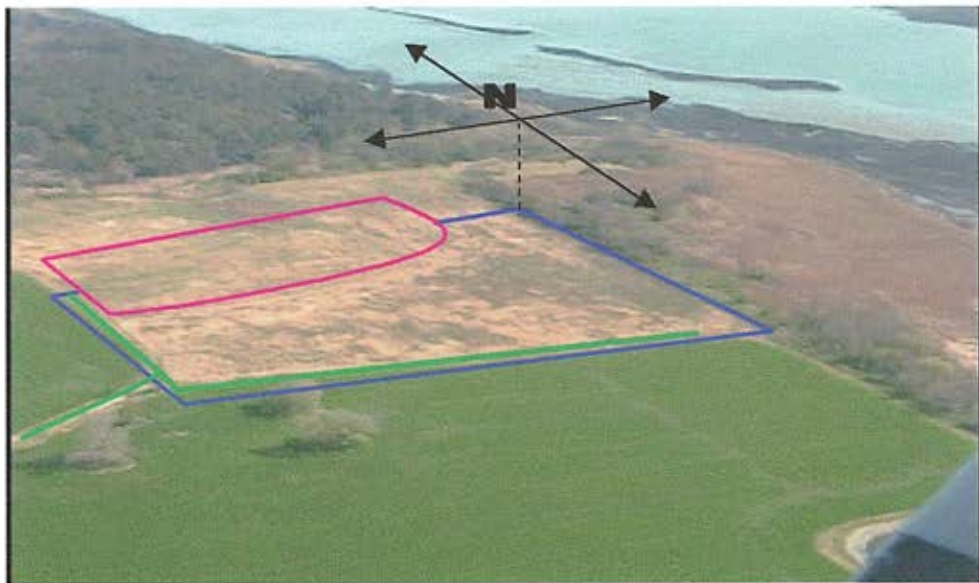


(b)

Figure 2-1. Location of the Oyster, VA Field Site. The series of enlargements starts with a map of the mid-Atlantic seaboard progressing to a photo of the field site (a-d). The dashed outlines on each image indicate the approximate area covered on the next enlargement. Maps obtained from MapQuest.com, Inc.



(c)



(d)

Figure 2-1. (continued). On photos (c) and (d) roads are outlined in green; the LTER field house is circled in orange; the borrow pit is highlighted in yellow; the field area is boxed in blue; and the tomato waste trenches are outlined in purple.

Over time the tomato leachate from the trenches has migrated down gradient across the study area and has served as a food source for aerobic microbes, producing an anoxic plume that extends into the field area.

C. Stratigraphy

The field site is located on the eastern side of the Central Upland of the Delmarva Peninsula, a peninsula composed of Tertiary and Quaternary deposits (Figure 2-2). The Delmarva Peninsula is composed of a series of Quaternary prograding spit deposits overlying claystone (Pliocene Yorktown Formation). At the Pliocene-Pleistocene contact an erosional unconformity suggests a rise in sea level after a period of exposure and erosion (Mixon, 1985). A major sea-level rise at 1.6 mya is also supported by chronostratigraphic data (Haq et al., 1988).

Before the major rise in sea level, the Susquehanna River flowed south in a north-south trending valley now occupied by the Chesapeake Bay. The valley divide to the east of the Susquehanna River was partly submerged at the time of Pleistocene sea-level rise. The portion of the ridge remaining above sea level served as an erosional headwall for the spit. The submerged portion of the ridge

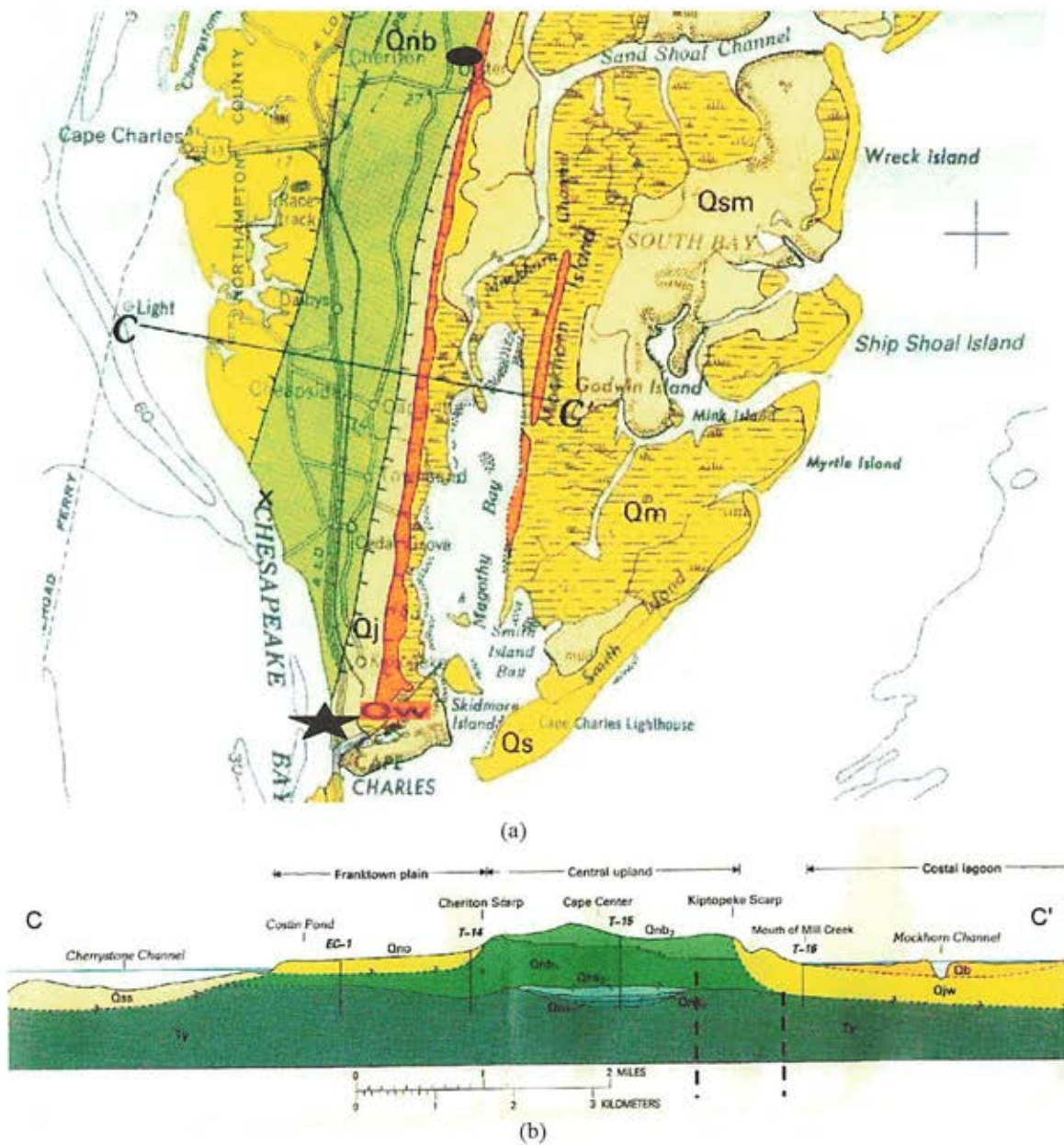


Figure 2-2. Geologic Map and Cross-Section of the Delmarva Peninsula. (a) The black oval indicates field area; the star indicates the location of an outcrop on a beach in Kiptopeke State Park. The symbols Qnb, Qj, and Qw represent the Nassawadox, Joynes Neck Sand, and the Wachapreague Formations, respectively. The other formations seen on the map and cross-section are of no importance to this study because they are not related directly to the field site. (b) A cross-section along C-C' shows the Kiptopeke scarp separating the Nassawadox and the Wachapreague Formations. The stratigraphy of the field site is similar to that between the dashed lines on the cross-section. Note that Qjw indicates the undifferentiated Joynes Neck/Wachapreague Formation (from *Mixon, 1985*).

served as the platform on which the spit was built (Oertel, 1987; Mixon, 1985).

Spit deposits are typically composed of a seaward beach facies and a landward lagoonal facies (Oertel, 1987). Sea-level rises allowed elongation of the spit. Four major periods of spit progradation are preserved as packages of stratified sand bounded by erosional surfaces, forming scarps at the ground surface (Mixon, 1985). The north-south trending Kiptopeke scarp can be observed in the western portion of the field area.

The Joynes Neck Sand lies above the Nassawadox Formation at an outcrop located just north of Kiptopeke State Park along the beach (Figure 2-3). The Wachapreague Formation and the Joynes Neck Sand are lithologically similar because of the close similarity in paleoenvironments (Mixon, 1985). The Nassawadox is a gold-grey, thin, slightly dipping, parallel-laminated, quartz arenite deposited in a beach environment. The Joynes Neck Sand is an orange-grey, cross-bedded, quartz arenite containing lag beds whose mineral grains have been coated with iron oxide, suggestive of nearshore fluvial deposits. The Nassawadox Formation in the western half of the field and the Wachapreague Formation in the eastern half of the

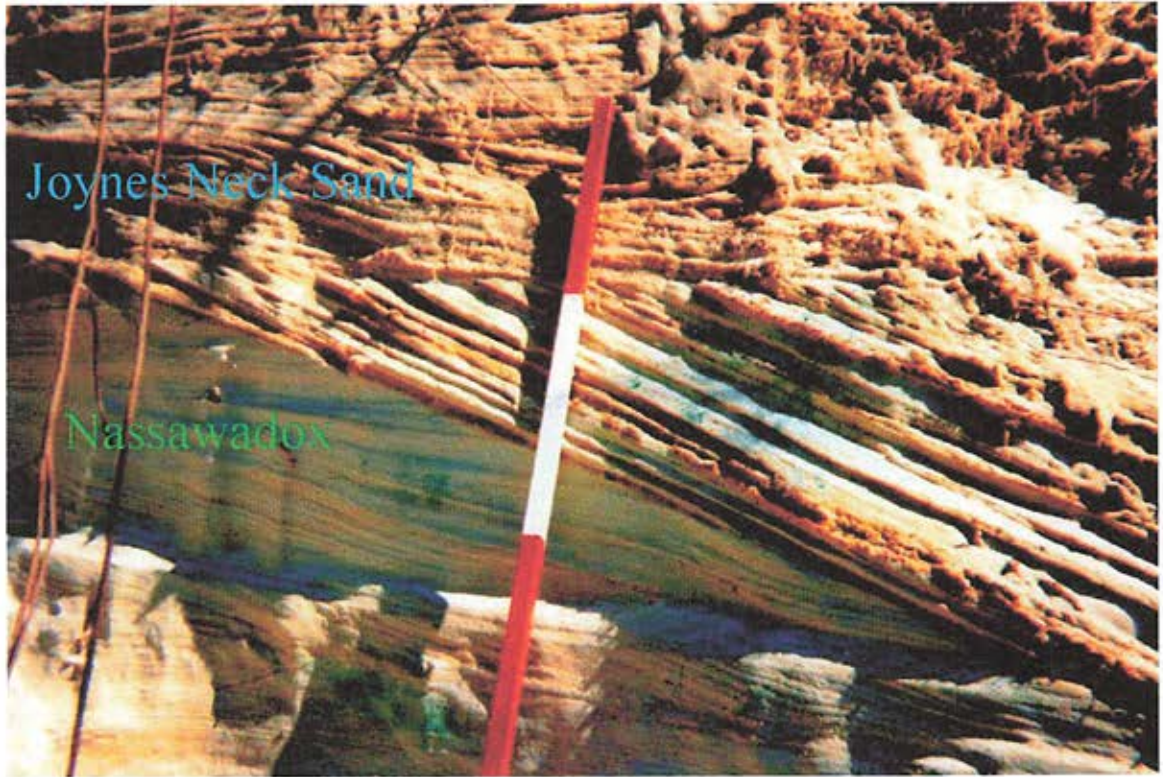


Figure 2-3. Exposure of the Nassawadox/Wachapreague Contact at Kiptopeke State Park. Here the Wachapreague equivalent, the Joynes Neck Sand, lies above the Nassawadox Formation. Notice the parallel laminae of the Nassawadox and the large-scale cross-bedding in the Joynes Neck Sand. The measurement stick is marked in 1 ft sections.

field are the two lithologies present at the site (Figure 2-4).

Based on observations made at a borrow pit approximately one-quarter mile to the south along strike from the field area, the subsurface of the field site consists primarily of clean, unconsolidated, fine to coarse, yellow, quartz sand from both the Nassawadox and Wachapreague Formations. Mineralogical analysis of the sand yielded less than 5% clays (Mills and Powelson, 1998). An aerial radiometric survey also indicated that the near-surface sand is relatively clean, containing minor amounts of clay (Kosanke, 1980).

B. D. Previous Studies

Aaron Mills and co-workers from the University of Virginia/Coastal Research Center (UVA/CRC) and the Department of Energy/Subsurface Science Program (DOE/SSP), have conducted a number of biogeochemical studies at the field site (Belitz and Burger, 1997; Knapp and Thompson, 1998; Mills and Powelson, 1998; Bolster et al., 1999). The DOE picked the site based on three characteristics: simple hydrogeology; homogeneity of the subsurface; and proximity to a field house, which is the headquarters and laboratory for the VCR/LTER. The DOE study involved injecting tracers,

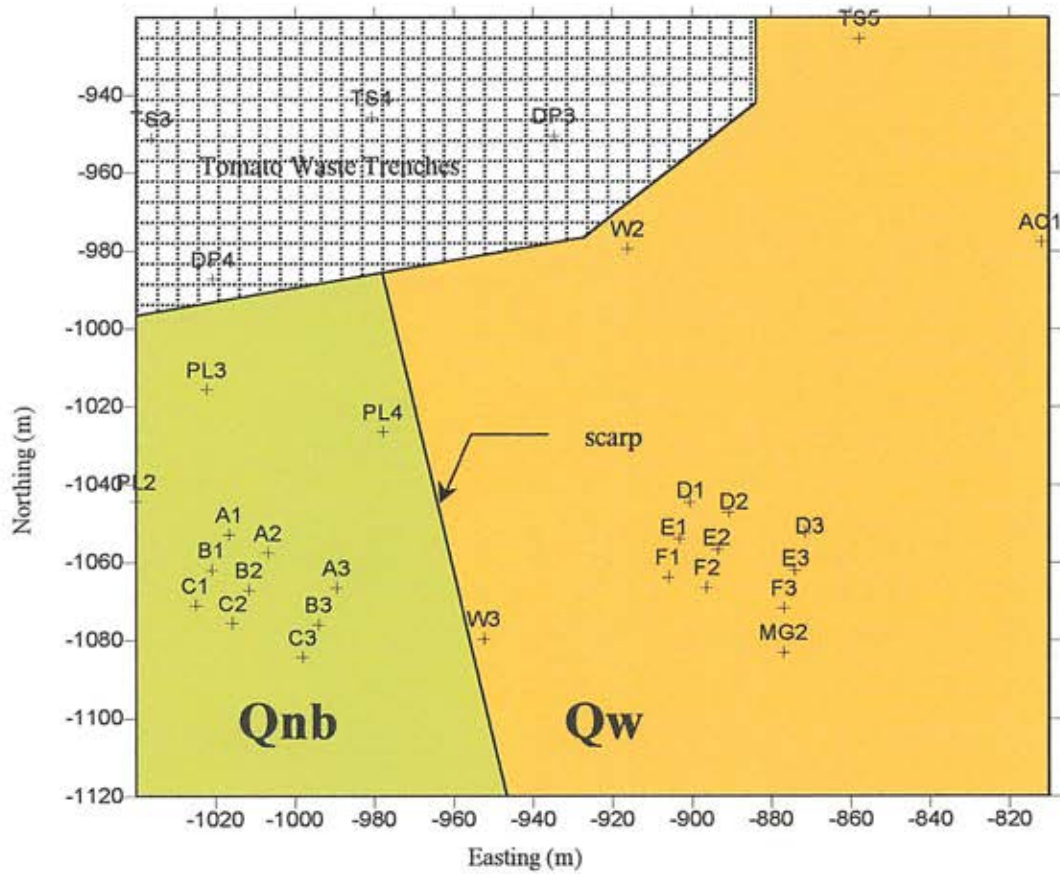


Figure 2-4. Geology of the Field Site. A scarp present on the surface identified the location of the contact between the Nassawadox (Qnb) and the Wachapreague (Qw) Formations. The crosses represent the wells, and their corresponding VCR/LTER and DOE labels. The patterned area represents trenches filled with tomato waste.

both Br⁻ and indigenous bacteria, into multi-level sampling wells emplaced at the field site to determine the hydrologic characteristics of the site and to contrast the transport of a chemical versus microbes in the subsurface media. DOE breakthrough curves showed that the Br⁻ tracer broke through sooner than the microbes and that less than one percent of the microbes actually broke through.

Data from the DOE study indicated that the field area contained two separate zones of differing groundwater biogeochemistry: an anaerobic zone representing a reducing environment; and an aerobic zone representing an oxidizing environment (Table 2-1).

Table 2-1. Summarized Biogeochemical Data (from Knapp, 1998).

Groundwater Parameters	Aerobic Zone	Anaerobic Zone
pH	5.3-6.5	5.9-6.6
Dissolved Organic Carbon (mg/L)	1.72-4.47	2.22-5.86
Dissolved Oxygen (mg/L)	5.0-10.6	0.05-0.9
Dissolved Ferrous Iron (mg/L)	0.0001-0.01	12.9-46.9
Nitrate (mg/L)	40-50	0-1
Extractable Ferric Iron (µm/g)	3.1-5.2	0.9-2.4

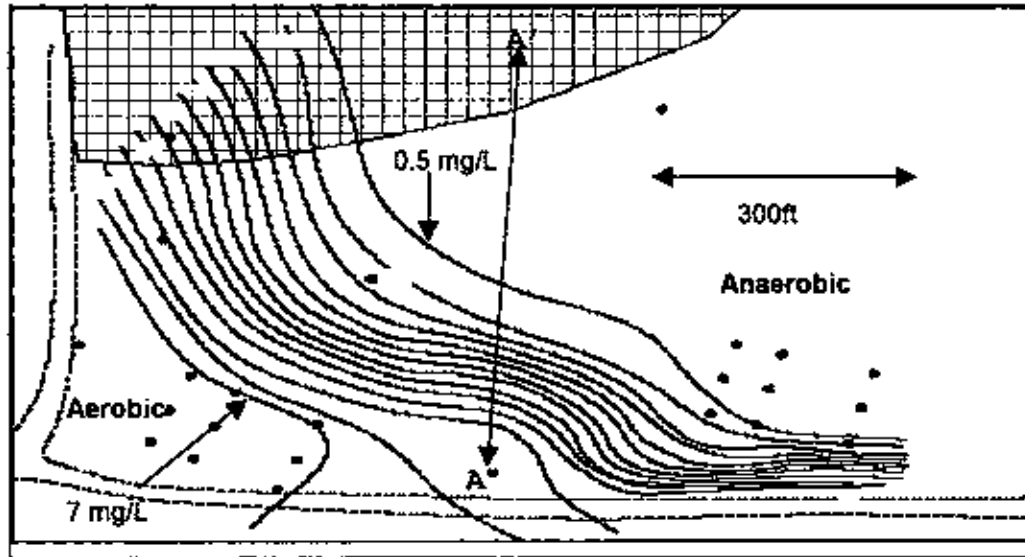
Under reducing conditions, ferric iron (Fe³⁺) becomes ferrous iron (Fe²⁺); under oxidizing conditions ferrous iron becomes ferric iron and precipitates. The anaerobic portion of the field has higher ferrous iron values than

the aerobic portion. The aerobic portion of the field has higher extractable ferric iron values than the anaerobic portion. Small amounts of nitrate in the anaerobic zone, compared to the aerobic zone, is further evidence that a zone of reduction is present (nitrate reduces to nitrite).

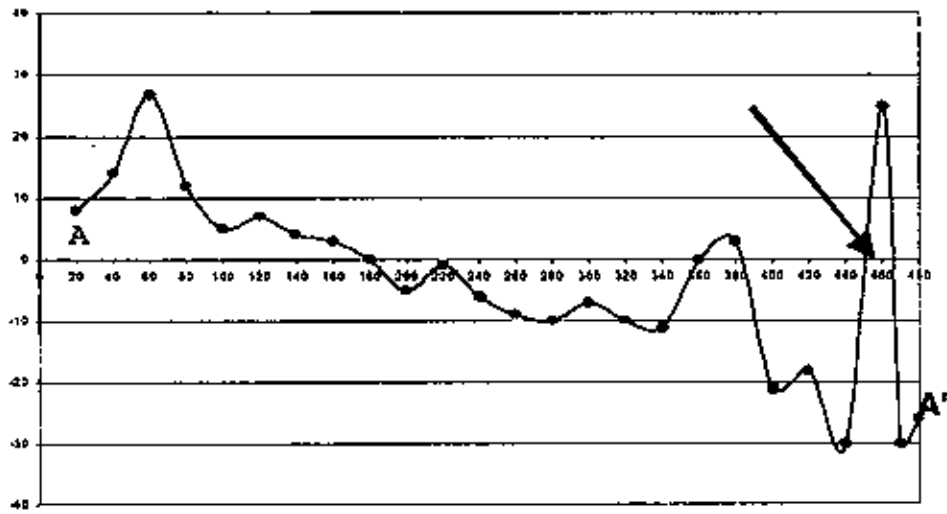
High dissolved organic carbon (DOC) in the anaerobic portion of the field indicates that tomato leachate is present. Where there is leachate, there are microbes using it as a food source, thereby reducing oxygen; the reduction of oxygen leads to anaerobic conditions. Therefore dissolved oxygen is a reliable indication of the shape and extent of the redox plume.

E. Preliminary SP Study

To decide whether to proceed with the study, I conducted a preliminary SP survey at the site with the help of my advisor Dr. Jonathan Nyquist in April, 1998. Based on the contoured DO (Knapp and Thompson, 1998), I decided to run a SP line across the redox boundary (Figure 2-5). The SP procedure discussed in Chapter 1 was followed except that the positive lead from the voltmeter was attached to the base electrode. This lead reversal resulted in a positive correlation between SP and redox and not a negative correlation, as seen in later surveys.



(a)



(b)

Figure 2-5. Results of the Preliminary SP Survey. (a) Shows the survey line (A-A') taken across the redox boundary as defined by contoured DO data from Mills (1998). The 7 mg/L and 0.5 mg/L DO contours are labeled; the contour interval is 0.5 mg/L. The patterned area contains trenches filled with the tomato waste. Dots indicate well locations. (b) Shows the plotted SP data from SP measurements taken every 20 ft along line A-A'. Notice the SP values decrease going from the aerobic zone to the anaerobic zone, except over the trenches, where heterogeneous surface conditions are present.

There was an overall trend to the SP data: low SP voltages correlated to reducing, anaerobic environments; high SP voltages correlated to oxidizing, aerobic environments. This positive correlation encouraged me to proceed with the investigation of the correlation between redox conditions and SP.

CHAPTER 3

MEASUREMENT OF REDOX CONDITIONS

A. Objectives

The purpose of mapping the shape and extent of the redox plume at the Oyster, VA field site was to compare it to the mapped SP. If the two maps mimicked each other, the hypothesis that SP can be used to monitor a redox plume would be supported.

B. Methods

First I tried to map redox conditions by taking direct measurements of redox potentials in groundwater from various wells using a peristaltic pump, a flow cell, and an Eh electrode. Three groundwater samples were measured at wells A3, W2 and D3 (refer to Figure 2-4) at three separate times during the morning of June 22, 1998 (Table 3-1).

Table 3-1. Eh Measurements from Wells

Wells	Eh1	Eh2	Eh3
A3	-256 mV	-265 mV	-232 mV
W2	-274 mV	-248 mV	-243 mV
D3	-243 mV	-223 mV	-267 mV

The data indicated that field measurements of Eh were unstable and irreproducible. Unstable and irreproducible Eh measurements made in groundwater are explained by the existence of competing redox couples creating a solution that is in constant chemical disequilibrium (Lindberg and Runnells, 1984). Because Eh proved unreliable for mapping redox conditions I used dissolved oxygen as an alternative parameter.

Although dissolved oxygen values do not indicate the full range of redox conditions, they are a good indicator of zones of reduction because oxygen is typically consumed by bacteria first under reducing conditions. Dissolved oxygen (DO) data collected from all the wells in the field area were contoured to make a map of DO zones. Low DO values indicate areas where the oxygen has been depleted through redox reactions in the groundwater.

A biologically mediated redox plume emanates from the tomato trenches. Organic contaminants, such as tomato waste, are typically in a reduced state (Engesgaard and Kipp, 1987; Christensen et al., 1989; Fetter, 1993) compared to background redox conditions. The contaminant can be used as an energy source by aerobic microbes through a series of biologically mediated redox reactions. Aerobic

heterotrophs make up the majority of the microbes present in the groundwater at Oyster, Va. (Mills and Powelson, 1998). These microbes use oxygen to obtain energy from the contaminant. Areas of low dissolved oxygen and high dissolved organic carbon (DOC) indicate the extent of the biogenetic redox plume and thus the corresponding contaminant plume.

Measurement of DO in well water required that exposure to atmospheric oxygen be kept to a minimum to get accurate values for DO in the groundwater. Keeping exposure to atmospheric oxygen at a minimum was done by pumping groundwater, using a peristaltic pump, into a cup which would receive the pump's output at its base while losing water by continuous overflow (Figure 3-1). A groundwater sample from the base of the cup would have the lowest exposure time to atmospheric oxygen. DO was measured using a CHEMET™. By comparing the color of the expended CHEMET™ to a color chart I was able to delineate DO values between 1 and 8 mg/L within a +/- 0.5 mg/L certainty (Figure 3-2).

I collected DO measurements in a single day, July 17, 1998, to avoid fluctuations in groundwater temperature, freshwater influx, and head. Values were then contoured using Surfer™, version 5.01, by Golden Software, after they

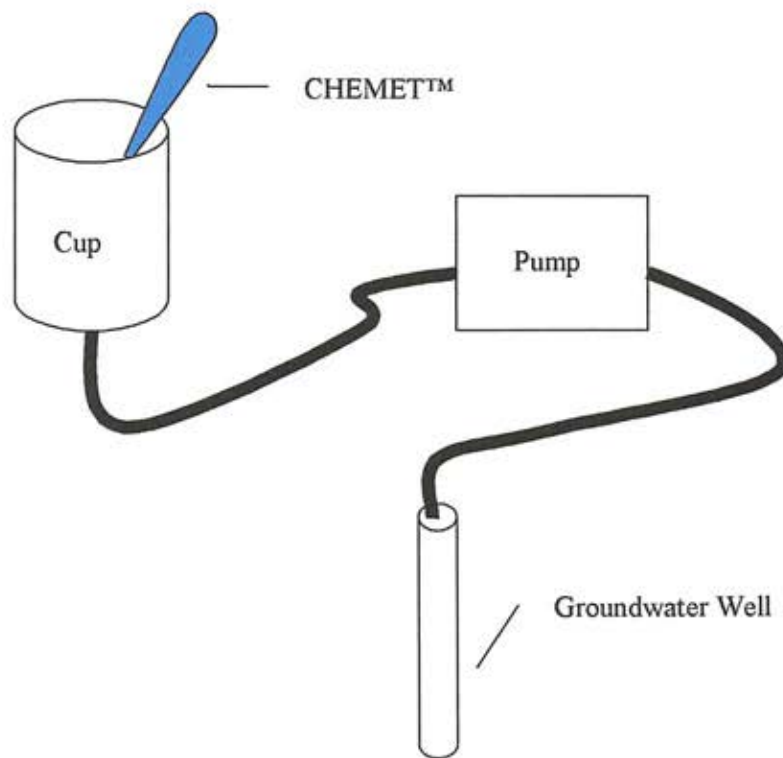


Figure 3-1. Equipment Setup for Collecting DO Data. Using a peristaltic pump, groundwater was pumped into the cup. The DO was measured from the base of the cup, using a CHEMET™, after five minutes of pumping.

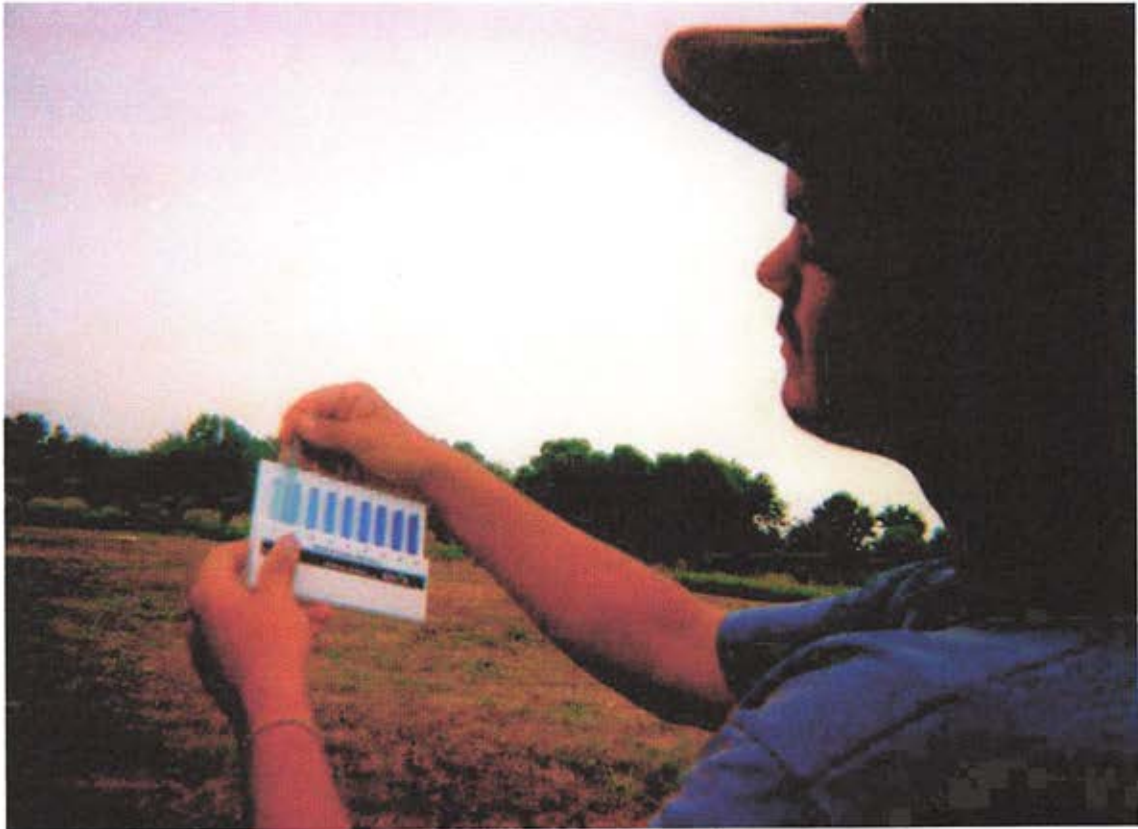


Figure 3-2. DO Measurements Using a CHEMET™. The geologist is comparing an expended CHEMET™ to the color scale to discern the DO of the groundwater sample. DO measurements were made at all the wells in the field area.

were interpolated onto a grid using kriging with the gridding parameters set to their default values (quadrant search, data per sector=6, minimum total data=5, maximum empty sector=4, radius1=138, radius2=138 and angle=0).

C. Results

The contoured data indicated a clear contrast in DO values over the field area (Figure 3-3). Generally aerobic conditions are present in the southwestern portion of the field and anaerobic conditions are present in the northeastern portion of the field.

There is an anaerobic plume, below 1 mg/L of DO, present in the groundwater flowing down piezometric gradient from the trench area. The DO ranges from 0.5 to 8 mg/L over ~100 m as the groundwater goes from reducing to oxidizing away from the center of the plume.

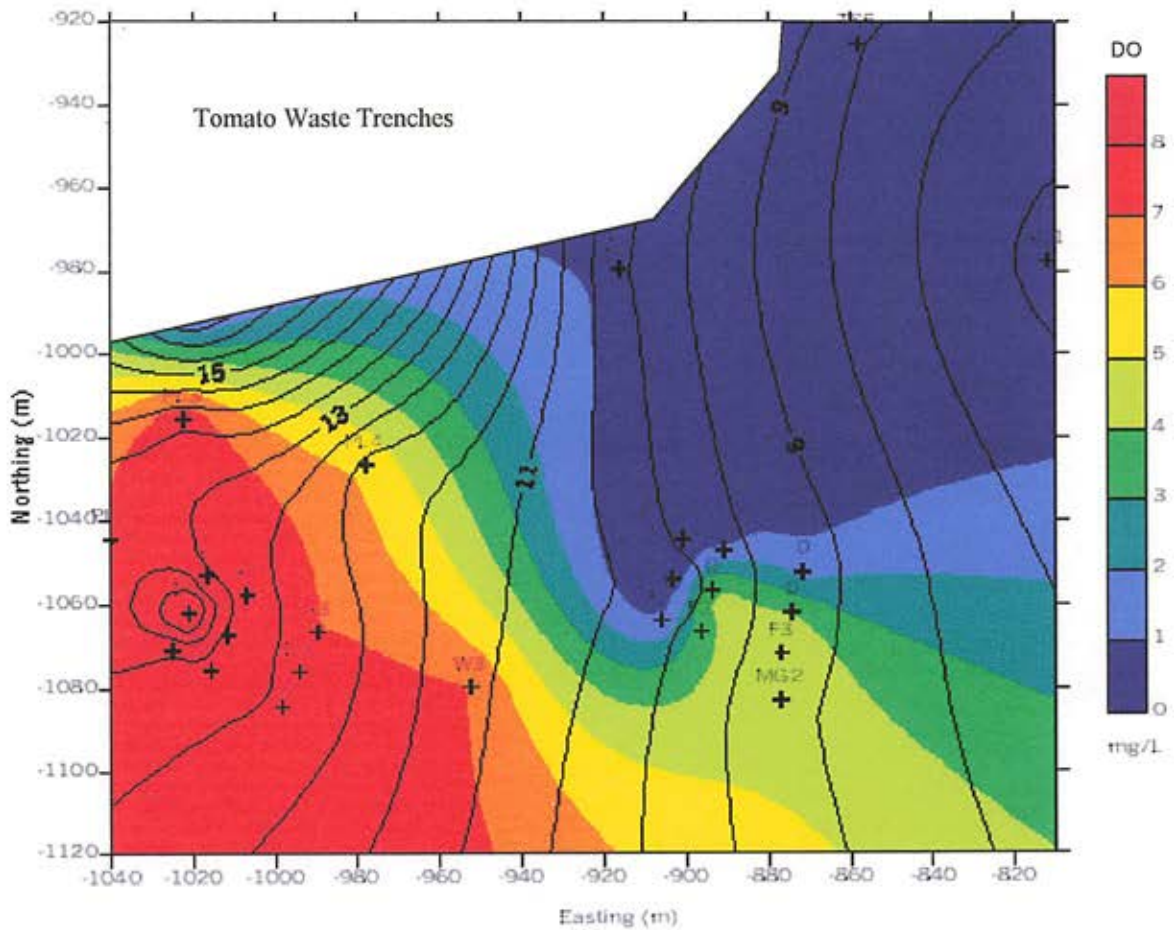


Figure 3-3. Contoured DO and Head Map. The color-filled contours represent the DO in mg/L. DO concentrations lower than 0.5 mg/L are shaded in white. The solid contour lines represent head levels in meters above sea level in 0.5 m contour intervals. The crosses represent the wells, and their corresponding VCR/LTER and DOE labels, from which samples were taken. The overall direction of groundwater flow is to the east.

CHAPTER 4

BACKGROUND GEOPHYSICAL SURVEYING

A. Objectives

I conducted magnetic, resistivity, and GPR studies at the field site to discover whether heterogeneities in the subsurface influenced the SP data. The redox plume would be mirrored by the contoured SP data only if the ground were reasonably homogeneous and devoid of cultural artifacts. Suspected heterogeneities at the Oyster field site included the two lithologies present and the possibility of a buried farmhouse foundation.

B. The Survey Grid

I surveyed a series of coordinate points over the field area using the same coordinate system the VCR/LTER researchers used for locating their wells. Using the same coordinate system allowed me to accurately superimpose data collected from the wells on the geophysical data. A metal stake in the northwestern portion of the field area was used as the origin. Coordinate points were labeled according to their distance south and east of this metal stake. On the resulting maps, (y) values increase northward and (x) values increase eastward. I discovered

later that the VCR/LTER grid system was surveyed without correcting for magnetic declination (12° west). To overlap the data sets I rotated my coordinate values 12° west about the origin.

C. Magnetic Survey

i. Objectives

The purpose of the magnetic study was to detect any iron in the subsurface at the field site. Though the area is currently undeveloped, scientists from Lawrence Livermore National Laboratory believed that the foundation of an abandoned farmhouse might be present.

Buried metal can influence SP data measured at the surface in two ways. The corrosion of metal in the subsurface is a redox reaction that creates its own SP signal. Metals can also warp SP equipotential lines surrounding a redox plume by creating a preferential path for electrical current. Mapping warped SP equipotentials would misrepresent the redox plume extent and shape. Consequently, it was important to know the location of any buried metal objects on site.

ii. Methods

Magnetometry is the standard method for detecting subsurface metal. Iron has a large magnetic susceptibility

compared to geological materials (Table 4-1). The detection limit depends on the mass of the target, the distance of target to the magnetometer, the magnetic susceptibility of the local geology, and the sensitivity of the magnetometer.

Table 4-1. Magnetic Susceptibilities of Various Materials (from Reynolds, 1997).

Material	Susceptibility (SI)
sandstone	0-21,000
shale	60-18,600
limestone	10-25,000
granite	10-65
basalt	500-182,000
iron	100,000-1,000,000

I used an OMNI IV proton precession magnetometer (Scintrix), with an accuracy of 1 nT, to conduct the magnetic survey. This unit was configured as a magnetic gradiometer. A proton precession magnetometer measures the total strength of the Earth's magnetic field. A gradiometer consists of two magnetometers vertically separated by a fixed distance (0.5 m for the OMNI IV). The difference in the field strength between the two sensors is the vertical magnetic gradient. Because changes in the Earth's magnetic field influence both magnetometers equally, the effects of magnetic storm activity or diurnal variations in the Earth's magnetic field do not require a correction.

At the field site, the magnetic field is nearly uniform because the subsurface is homogeneous sand. Because sand has an extremely low magnetic susceptibility compared to iron metal (refer to Table 4-1), any magnetic anomaly must be attributed to local metal objects. Metal not containing iron cannot be detected with a gradiometer, but because most metals contain at least some iron, it is unlikely that a farmhouse foundation would go undetected.

The appropriate survey line spacing depends on the size of the target. Tighter spacing improves resolution but requires more measurements and more time. For this study I picked a line spacing that would detect a 100-pound iron mass, above the 1 nT threshold of the gradiometer, from the most remote point from any survey point. Based on a nanogram (Breiner, 1973) that plotted the magnetic strength of an object versus distance from a measuring point (Figure 4-1), I could detect a 100-pound iron mass as a 5 nT anomaly from 25 feet away. Lines -1000E through -850E were used to collect vertical magnetic gradient data. The spacing of measurement points along each line was 3 m. Objects that could not be detected with this grid spacing were either too small or too deep to influence the SP. The gradiometer

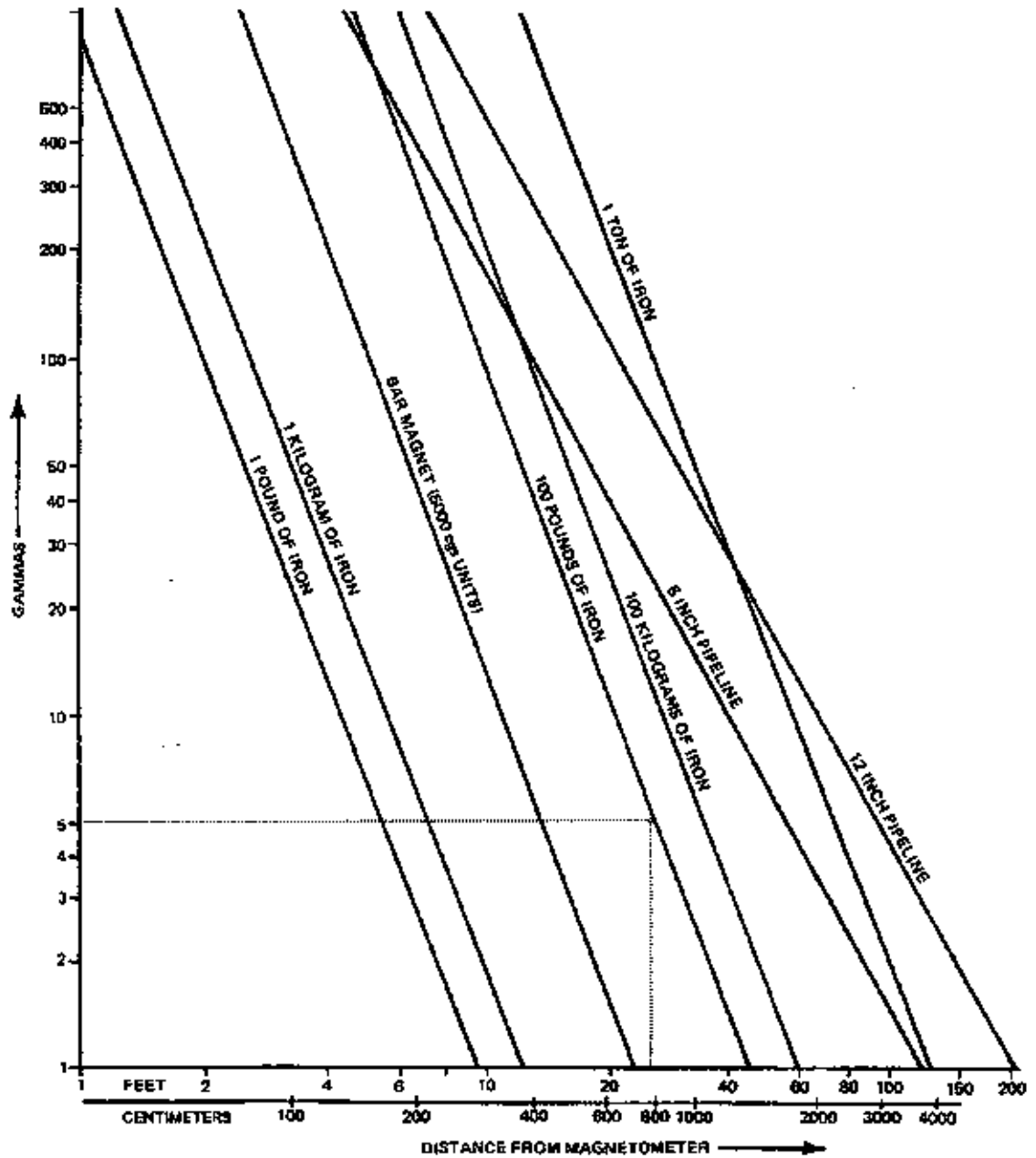


Figure 4-1. Magnetic Nonogram for Estimating Anomaly Magnitude.
 For example, for 100lbs of iron, the nonogram states that a 5 gamma (nT) anomaly is produced from any measuring point 25 ft away (from Breiner, 1973).

data were surface contoured for the field site using Surfer™. The interpolation scheme used was kriging with default settings (refer to pg. 30).

iii. Results

The vertical magnetic gradient survey revealed two anomalies in the field area (Figure 4-2). These anomalies can be explained by surface material. A metal casing over a well created the small anomaly in the southwestern portion of the field. The large anomaly in the northwest portion of the field area was produced by a photometer emplaced by the LTER researchers. Therefore, I concluded that the SP anomalies at the site are not related to the corrosion of subsurface ferrous metal, nor are ferrous metals distorting equipotential lines associated with the redox plume.

D. Resistivity Survey

i. Objective

The objective of the resistivity survey was to detect zones of varying electrical resistivity present at the field site. The field area is underlain by two formations that are mineralogically homogeneous but with different structures. If these two structures created two

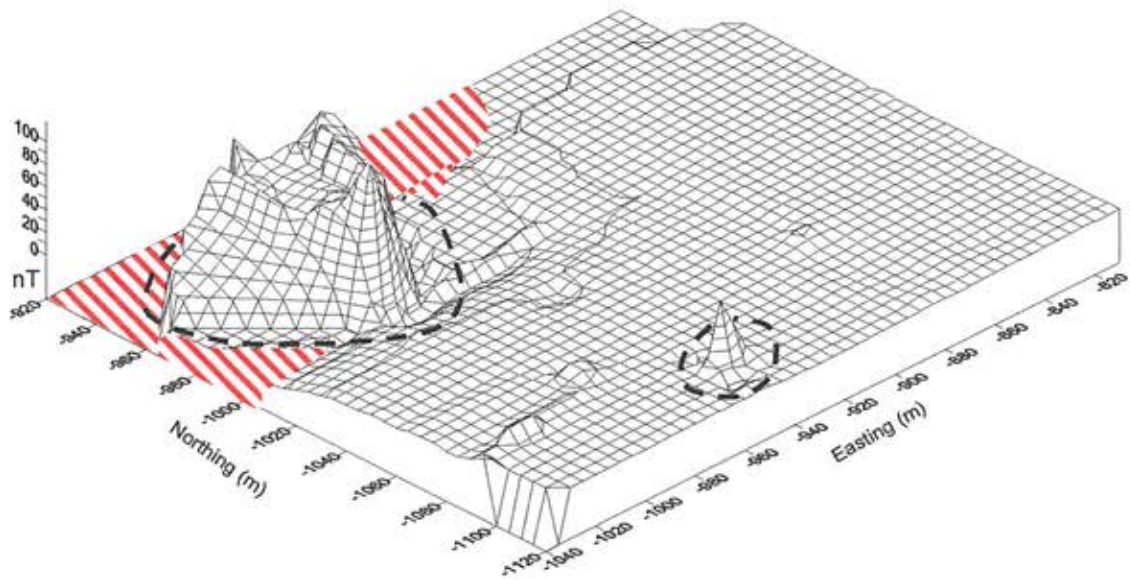


Figure 4-2. Vertical Magnetic Gradient Surface Map. Surface contoured gradiometer data yielded two hits (enclosed in the dashed areas) produced by two metal objects at the surface. The pin-stripped area indicates the location of the tomato waste trenches.

different zones of electrical resistivity it would have influenced the SP data.

Differing zones of electrical resistivity can influence SP data measured at the surface in two ways. These zones can create electrochemical potentials and they can warp equipotentials from a redox source. Consequently it was important to know the location of electrical heterogeneities.

ii. Methods

Resistivity surveys can be used to generate 2D-resistivity cross-sections of the subsurface beneath a survey line. A resistivity survey involves sending electrical current into the ground and recording the electrical resistance the current encounters at various distances between the source and the sink electrodes. The larger the spacing between the source and sink electrodes, the deeper resistivities can be measured. A Sting/Swift™, by Advanced Geosciences, Inc., multi-electrode (28 in total) resistivity unit was used to conduct the survey with a cable that permitted a maximum electrode spacing of 12 m.

In the past, resistivity surveys were quite tedious because of the repositioning of electrodes required for each measurement along the line. By using a multi-

electrode resistivity device, I was able to lay out a line of the appropriate length, plant the electrodes and allow the resistivity system to control the firing sequence of the electrodes.

The appropriate survey line spacing depends on the size of the target. I was specifically looking for changes associated with the Nassawadox/Wachapreague formational contact and the electrical structure between the water table and the surface. Three 98 m lines with a 3.5 m line spacing represented a good compromise between the amount of area to cover and the desired depth of penetration. Two lines ran parallel to strike within each formation and one ran perpendicular to strike crossing the contact between both formations (Figure 4-3).

Dr. Jonathan Nyquist and I ran all three resistivity lines on June 14, 1998. Apparent resistivities collected from the survey were processed, using an inverse modeling program called RES2DINV™, version 2.1, to produce 2D resistivity cross-sections (Loke and Barker, 1996)

iii. Results

Using the RES2DINV™, I processed all three survey lines (Figures 4-4, 4-5, and 4-6) The Sting was able to reach 20 meters in depth. Data sets for lines (1) and (2) show three

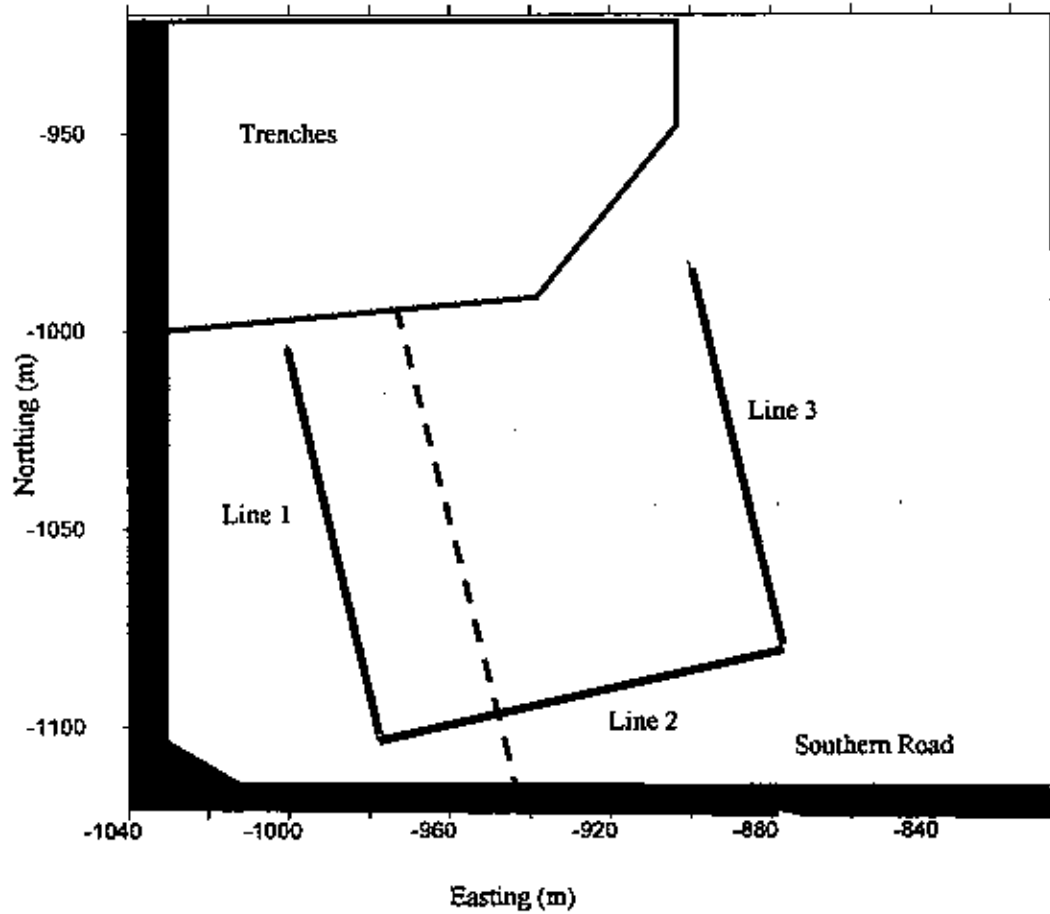


Figure 4-3. Location of Resistivity Survey Lines. Resistivity survey lines are labeled 1-3. The dashed line represents the scarp between the Nassawadox Formation, to the west, and the Wachapreague Formation, to the east. The thick black lines mark the roads west and south of the field site.

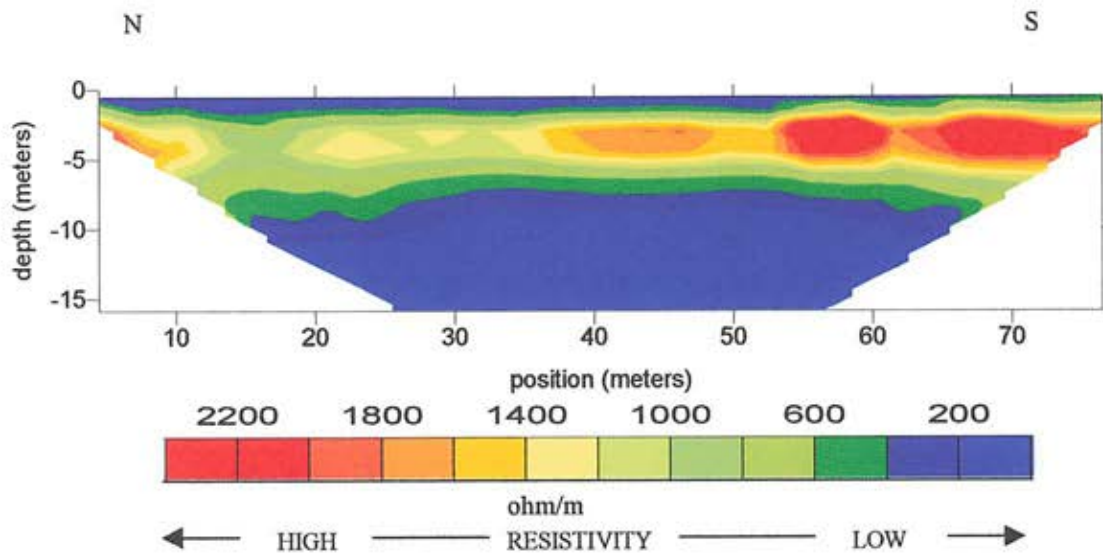


Figure 4-4. 2D-Resistivity Cross-Section Along Line 1. The cross-section shows three distinct zones of resistivity. Starting from the top these zones are: the soil layer, the zone of aeration, and the saturated zone.

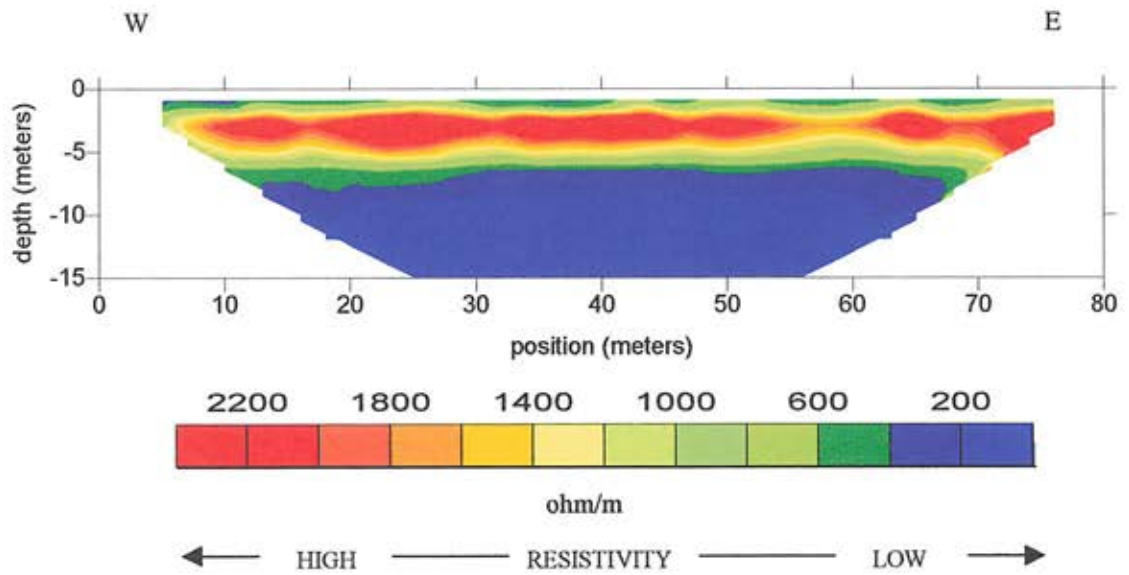


Figure 4-5. 2D-Resistivity Cross-Section Along Line 2. The cross-section shows the same three distinct zones of resistivity shown in Figure 4-4. Note the slight decrease in the thickness of the zone of aeration as you go down the piezometric gradient (toward the east).

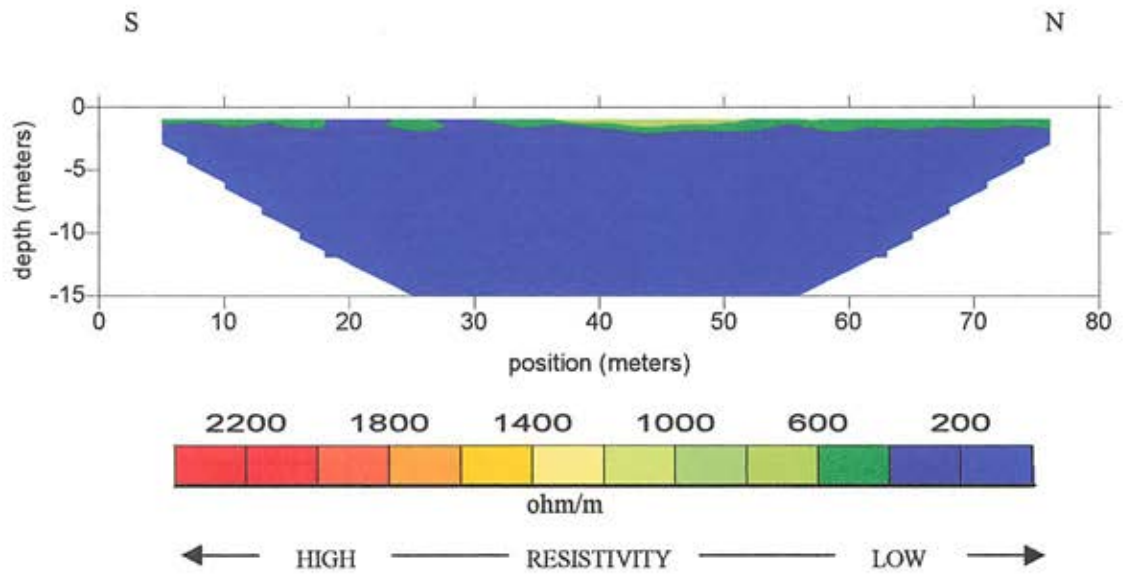


Figure 4-6. 2D-Resistivity Cross-Section Along Line 3. The cross-section shows only two of the three zones of resistivity (there is no noticeable zone of aeration) seen in Figures 4-4 and 4-5.

distinct zones of resistivity, while line (3) only shows two of the three zones. The three zones of resistivity are: a conductive layer at the surface, probably caused by moisture in the root zone; a resistive layer, probably caused by the zone of aeration, below the upper conductive layer; and a lower conductive zone probably caused by the zone of saturation. The resistivity survey along line (3) did not detect the zone of aeration because the water table is too close to the surface.

A near-surface water table is supported by the head data. A slight decrease in the thickness of the zone of aeration is noticeable along line (2), which ran down piezometric gradient. The resistivity data showed no lateral change in composition that could influence SP. The resistivity data did not show the formational change across the scarp indicating that the two formations present are electrically homogeneous despite the change in structure. The resistivity data also supported the hypothesis that SP values measured at the surface were not influenced by subsurface electrical heterogeneities.

E. Ground Penetrating Radar Survey

i. Objectives

The purpose of conducting a Ground Penetrating Radar (GPR) survey of the field site was to examine the subsurface structures present. GPR was used to confirm Mixon's assumption that the Joynes Neck Sand is lithologically similar to the Wachapreague Formation. GPR data were used to help pinpoint the Nassawadox/Wachapreague formational contact on the resistivity cross-sections, and to examine the changes across that boundary.

ii. Methods

GPR is used primarily to map near-subsurface geologic structure because GPR has the highest resolution of any geophysical tool; it also typically has the shallowest depth of penetration. The subsurface dielectric constant, electrical conductivity and the frequency of the radar antenna control the depth of penetration and resolution. Equation 4-1 can be used to estimate GPR penetration in meters if the subsurface resistivity is known:

$$d_{\max} = 35\rho/1000 \quad (4-1)$$

The resistivity of the subsurface is ρ .

Based on the resistivity survey data, the average near surface resistivity was determined to be 300 ohm/m. Using this value the depth of penetration is approximately 12 meters. The depth was calculated without a frequency component in the formula, but agrees with the results from the 100 MHz survey and is a slight underestimate compared to the results of the 250 MHz survey. Clean sands with low dielectric constants and low conductivities do not dampen GPR waves as much as lithologies with high dielectric constants and high conductivities. Thus GPR can penetrate clean sands to greater depths than can be reached in clay-rich sands.

The two antennas used for the survey were a 100 MHz and 250 MHz, Mala, Inc., radar units. The 100 MHz antenna resolved 20 cm beds to a depth of 10 m while the 250 MHz antenna resolved 9 cm beds to a depth of 6 m. These resolutions were calculated using an average velocity of a GPR wave through sand of 80 mm/sec (Reynolds, 1997). These depths encompassed the entire zone of saturation, which ranged from 2.25 ft to 7.75 ft, determined using head data from wells and the resistivity cross-sections. The resolution was adequate given the sizes of structures seen at the Kiptopeke State Park outcrop.

A gentle slope on the surface corresponding to a topographic scarp, visible along the southern road, trending north-south, 3 m wide and 0.5 m of relief, was assumed to be the Nassawadox/Wachapreague formational contact. To identify the differing structures of both formations I ran a GPR line perpendicular to the Nassawadox/Wachapreague formational contact along the southern road using the 100 MHz antenna (Figure 4-3). To examine the continuity of beds within a formation, I ran a GPR line parallel to strike within the Nassawadox using the 250 MHz antenna.

The raw GPR data collected were processed using GRADIX™ by Interpex. The following processes, in this order, were used to produce a GPR cross-section using the GRADIX program: set time zero, de-wow (removal of low frequency noise), band pass filter (80-400 MHz), and automatic gain control.

Results

Using GRADIX™, I processed the two GPR survey lines (Figures 4-7 and 4-8). The data show that the Nassawadox Formation and the Wachapreague Formations have different sedimentary fabrics. The Nassawadox Formation appears to be horizontally laminated while the Wachapreague Formation

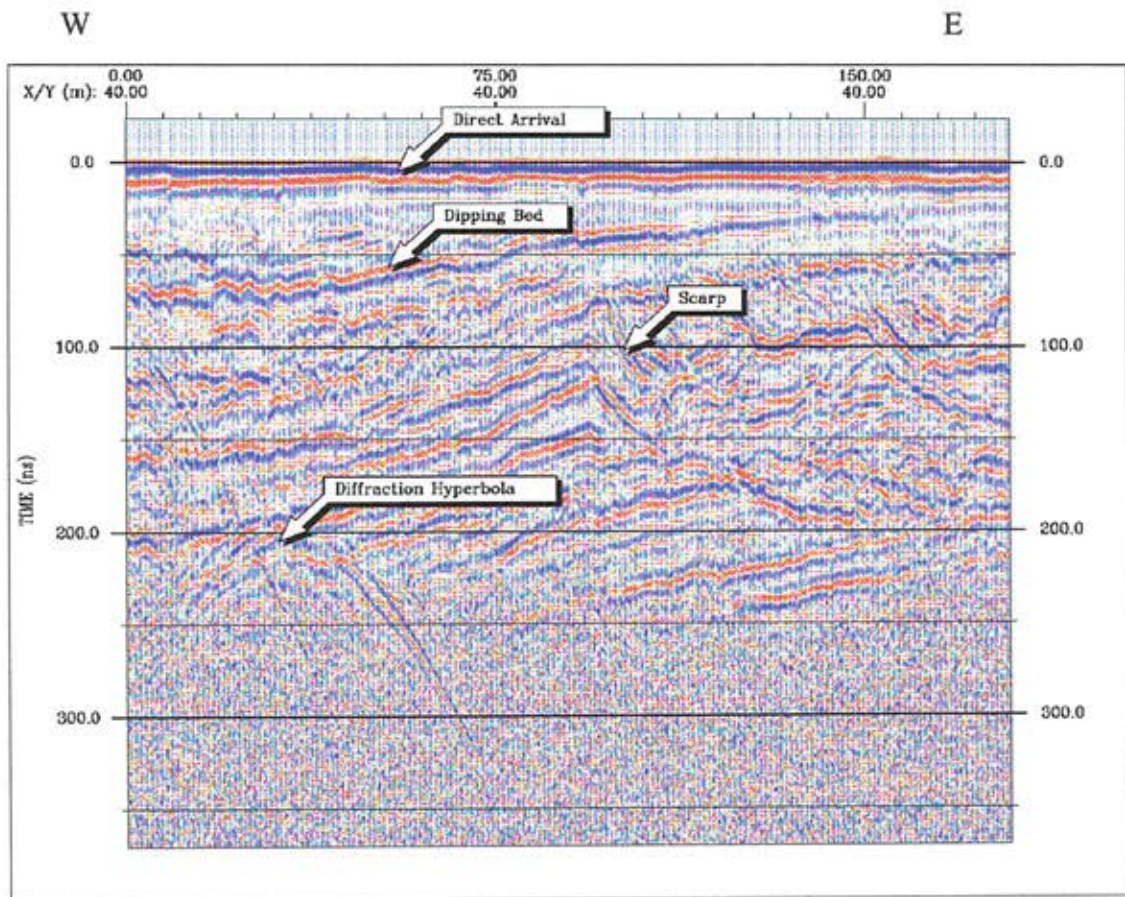


Figure 4-7. Results from the 100 MHz GPR Survey Along the Southern Road. The GPR line crosses the scarp separating the Nassawadox and the Wachapreague Formations. Notice the two differing structures east and west of the scarp. To the west of the scarp is the Nassawadox Formation, which contains laminar bedding; to the east of the scarp is the Wachapreague Formation, which contains cross-bedded fluvial channels. Individual cross-beds within the Wachapreague Formation are not discernible. The vertical scale is two-way travel time for the GPR wave in nanoseconds (ns). By assuming a GPR wave velocity of 80 mm/ns, through clean sands, the depth of penetration is approximately 10 meters, when using 250 ns for a two-way travel time.

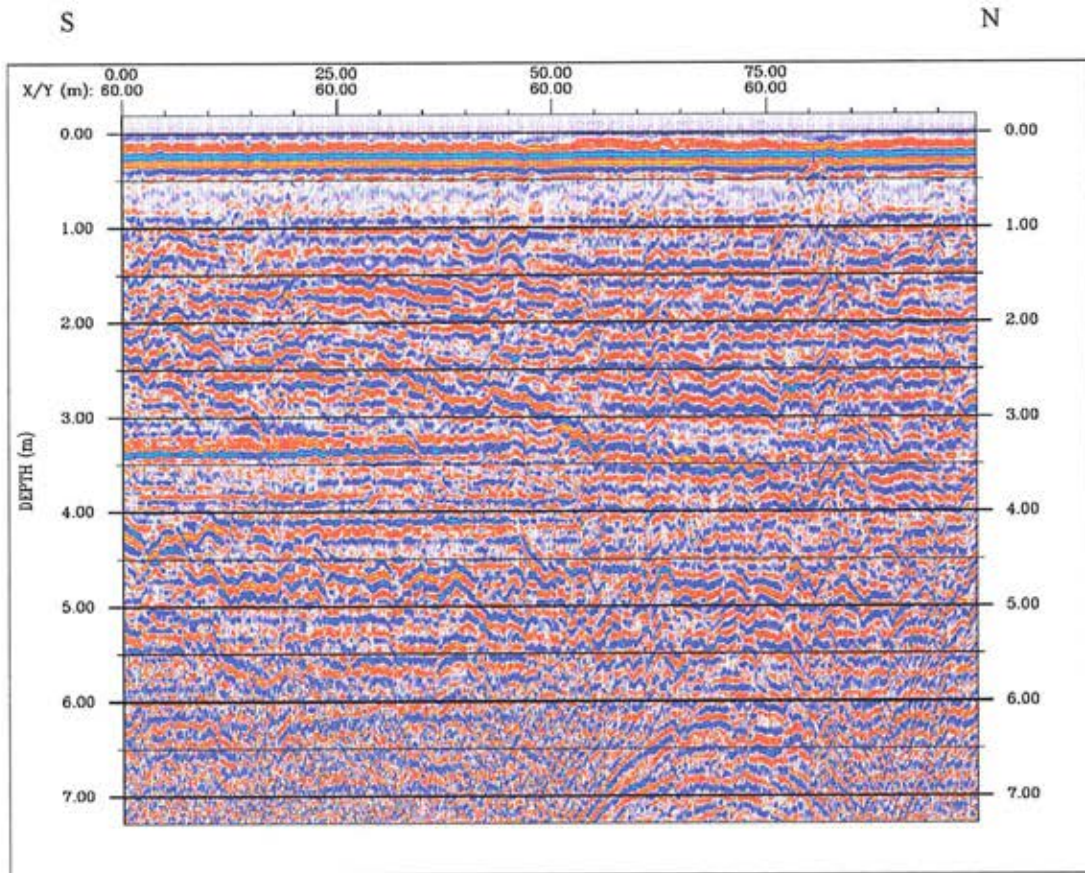


Figure 4-8. Results from the 250 MHz GPR Survey of the Nassawadox Formation Parallel to Strike. The GPR cross-section shows the continuity of laminated structures in the Nassawadox Formation. Depth of penetration is approximately 6 m.

is cross-bedded. The data also show that there is continuity of the sedimentary fabric along strike. These results agree with the observations made at the Kiptopeke outcrop and with Mixon's data. Further proof that the two formations have similar resistivities, and are electrically homogeneous, is the fact that the depth of penetration does not change much across the contact.

F. Conclusions of the Background Geophysical Surveying

The magnetometry data showed that no buried metal existed at the field site. The resistivity data showed that both formations were electrically homogeneous. Electrical homogeneity was also supported by the GPR data. All of the data support the assumption that the field site is underlain by relatively homogenous sand with the exception of sedimentary fabric. Based on the background geophysical surveying of the Oyster field site, I conclude that the SP data collected at the site were not influenced by cultural items buried in the subsurface, or by electrical changes between the two formations.

CHAPTER 5

SPONTANEOUS POTENTIAL STUDY

A. SP Objectives

The purpose of collecting SP measurements was to generate a contour map of SP data to compare with the contoured DO data. SP data were collected twice during the summer of 1998, once between June 26-29, and once on July 6, to determine the reproducibility of the results.

B. Methods

The background geophysical evidence indicated that the ground was homogeneous and would not influence SP. To monitor temporal variations during both surveys, I emplaced a data logger attached to two SP electrodes in the oxidizing zone, near the junction between the southern and eastern roads. The data logger measured SP between the two electrodes every half-hour. The accuracy of the data logger was +/- 1 mV. Fluctuations were never greater than 1 mV. Because fluctuations were minimal I dismissed temporal variations as a source of SP. The base electrode for both surveys was emplaced at -970E, -1030N. Contact resistances were recorded for each measurement to verify good soil to electrode contact. The first survey (SP1) was

done on the survey grid described in Chapter 4. Lines -1000E through -850E were sampled at 3 m intervals.

Lines collected for the second SP survey (SP2) were made at 5 m intervals between wells. The coordinates of the wells were measured by the UVA researchers. I calculated the coordinates of the measurement points between the wells by applying a trigonometric function to interpolate between two known endpoints. By using interpolated points I was able to select lines which crossed nearly perpendicular to the redox boundary. Line SP2 is more reliable than SP1 because I developed a more efficient method of collecting the data. SP1 was collected over a period of three days; I collected SP2 in one day. Collecting all of the data in one day reduced the effects of changing soil moisture and temperature. To cut down on the time required to collect SP data sets, I used a 50 cm diameter hand auger to dig holes rather than the rock hammer I used for SP1. I attached the voltmeter and roving electrode to a broom handle, allowing me to spear the roving electrode into freshly augured 30 cm deep holes with one hand while carrying the spool of in the other hand. Another student working at the LTER assisted by augering the holes.

I followed several important procedures to get accurate results for SP2. I kept three electrodes in a supersaturated cupric sulfate solution prior to the survey: the base electrode, the roving electrode, and the standardizing electrode. They were soaked in the bath until there was minor (< 5 mV) SP differences between them. The voltage potential between the roving electrode and the standardizing electrode was recorded and compared to the voltage potential between them after three survey lines were completed to see if there was any drift in electrode potentials. The maximum drift was ± 3 mV.

Previously measured points were checked periodically during the survey to test the accuracy of the data; repeat measurements never varied more than ± 5 mV from the previous measurement. Both data sets were interpolated and contoured using Surfer[™]. Kriging with default settings was used to grid the data (refer to pg.30h).

C. SP Results

Several methods were used to test whether changes in DO correlated with changes in SP values across a redox boundary. Both SP data sets show changes in SP across the redox boundary (Figure 5-1 & Figure 5-2). In the western portion of the field, on both maps, there are more negative

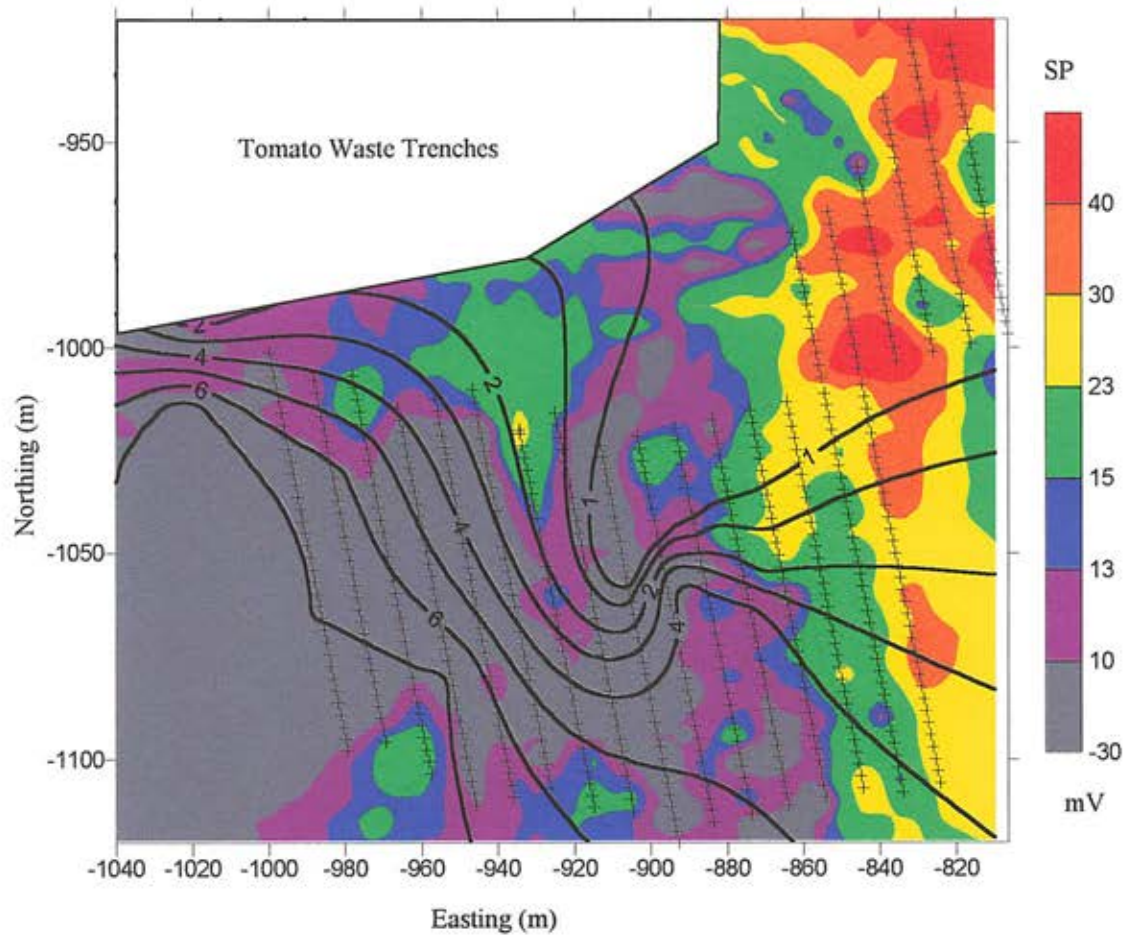


Figure 5-1. Contour Map of DO and SP1. The filled contours represent the SP values across the field area. The line contours represent DO in mg/L. The crosses represent the measurement points for SP2.

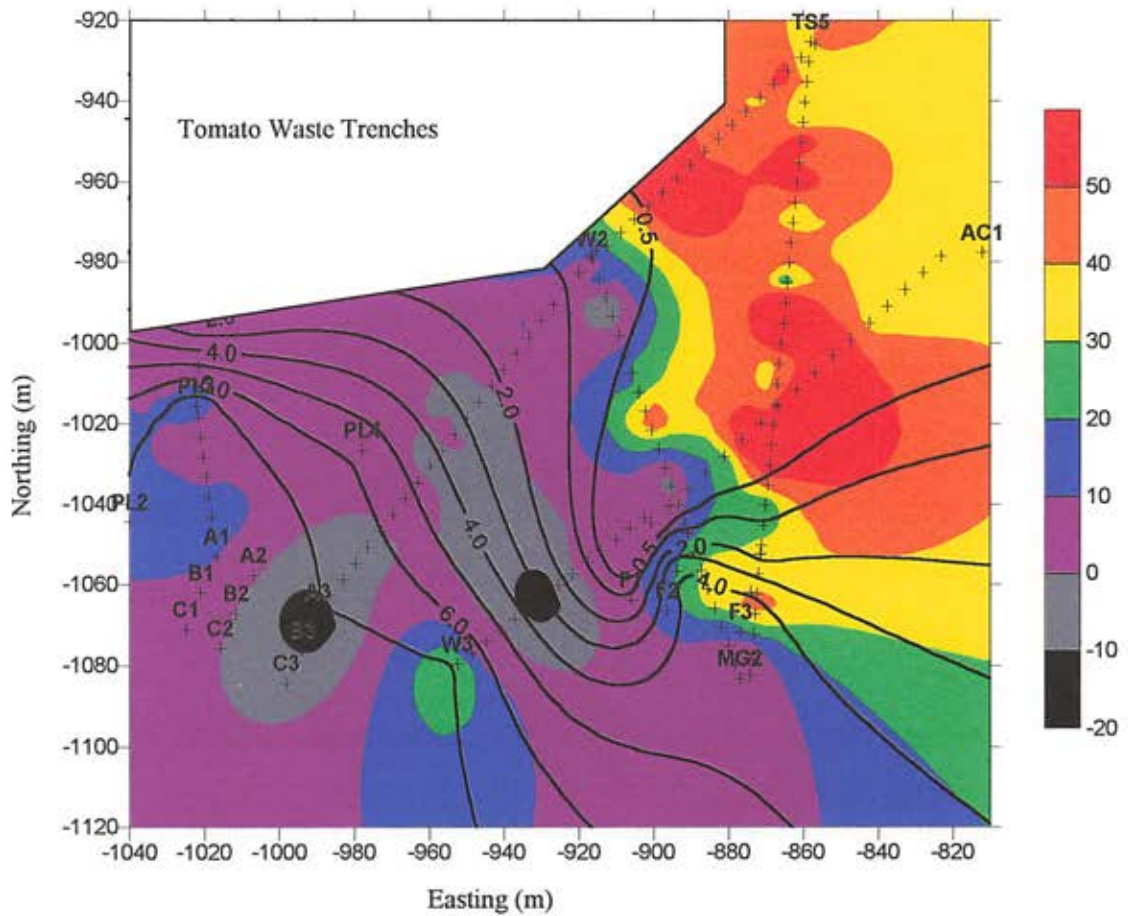
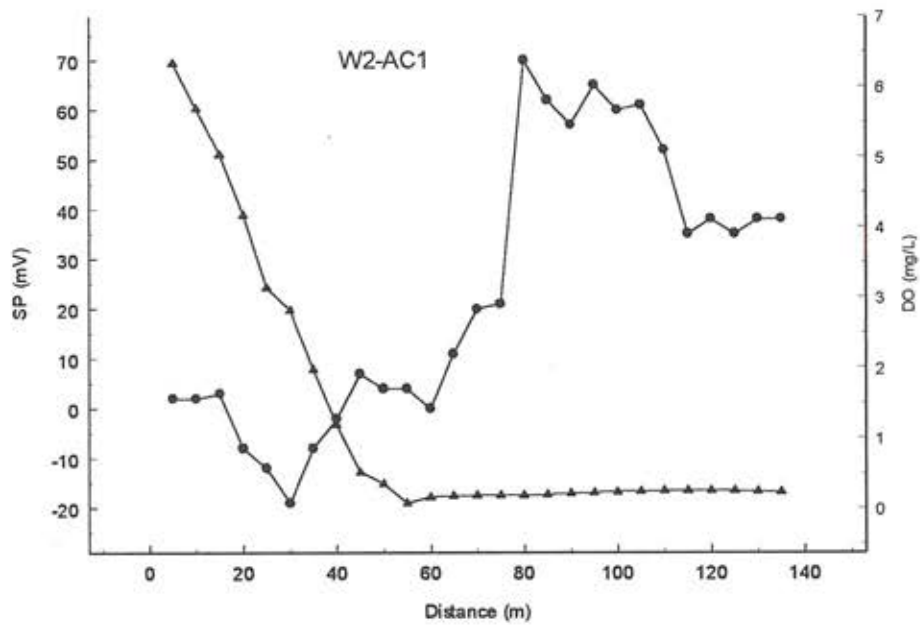


Figure 5-2. Contour Map of DO and SP2. The filled contours represent the SP values across the field area. The line contours represent DO in mg/L. The crosses represent the measurement points for SP2. Transects which cross perpendicular to the DO boundary are A3-TS5 and W2-AC1.

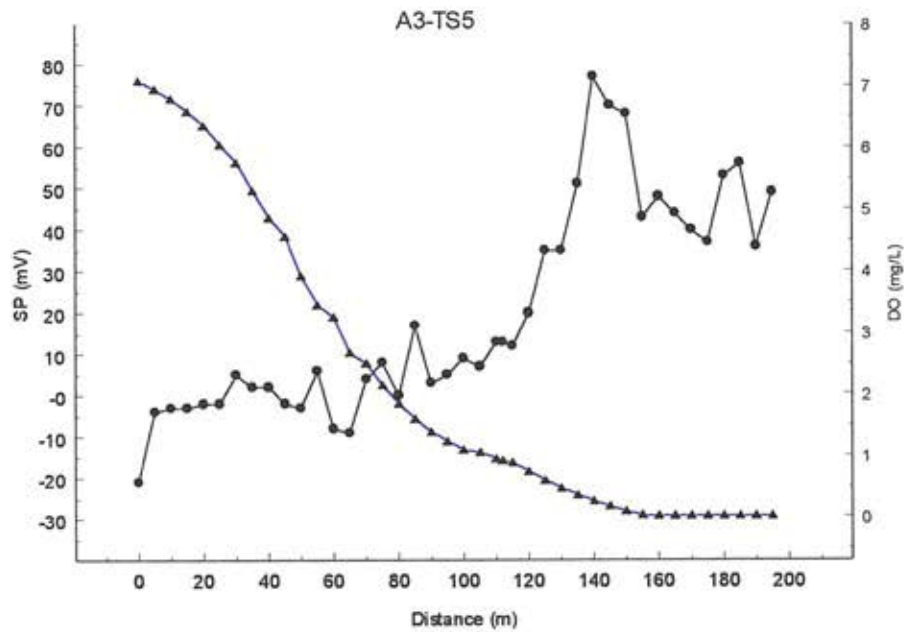
voltages compared to the more positive voltages in the eastern portion of the field. These zones of negative and positive voltages correspond well with the aerobic and anaerobic portions of the field area, respectively. The poorest fit is in the southeast corner where there are no wells to map the DO plume. SP values during the SP2 sampling event were higher because soils were drier and hotter later in the summer.

Another way I compared the SP and DO data sets, besides visually correlating the two contour maps, was to plot DO and SP versus transect position (Figure 5-3). To display the most apparent correlation, I used two lines that ran nearly perpendicular to the redox boundary. The DO data points on these lines were interpolated using slices of the Kriged contours. There is definite negative correlation between SP and DO; increasing DO results in decreasing SP and vice versa. For DO values less than ~2 mg/L there is a strong negative correlation between the two parameters; for DO values above ~2 mg/L SP remains constant with relation to DO (Figure 5-4).

Because the data were not normally distributed, a parametric statistical analysis is not valid. However, the non-parametric Spearman rank correlation analysis (Conover,



(a)



(b)

Figure 5-3. Plot of DO and SP Versus Distance for W2-AC1 & A3-TS5. DO is represented by the connected triangles; SP is represented as the connected circles. Notice the inverse relationship between DO and SP.

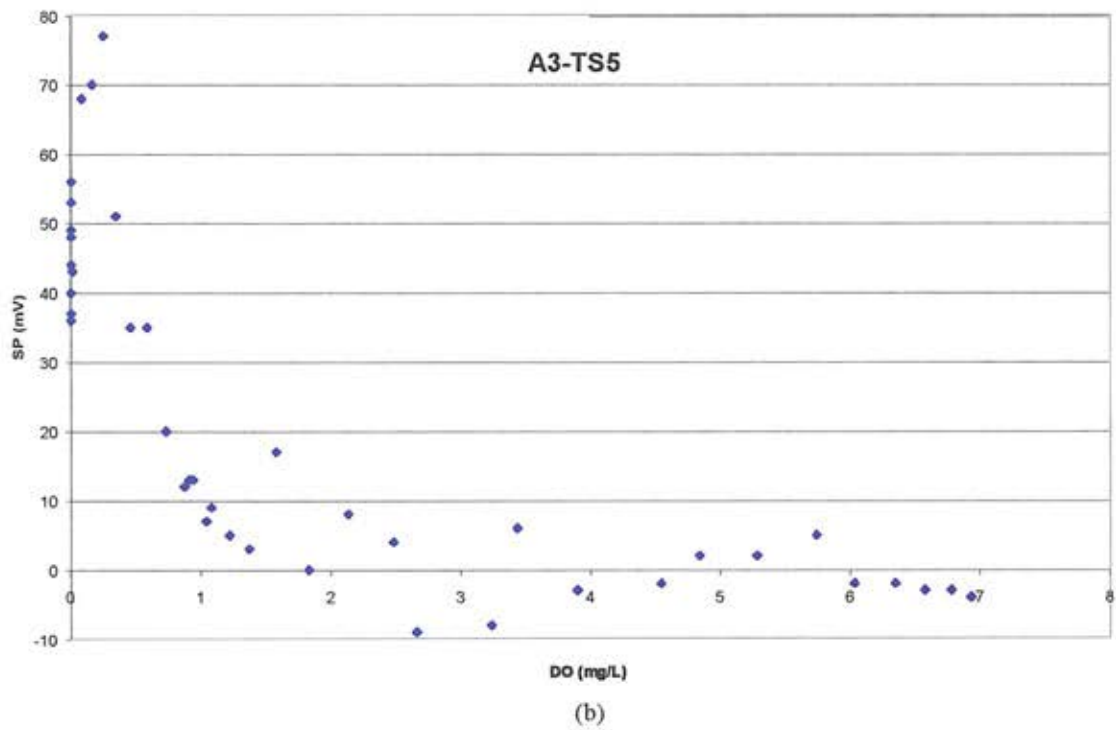
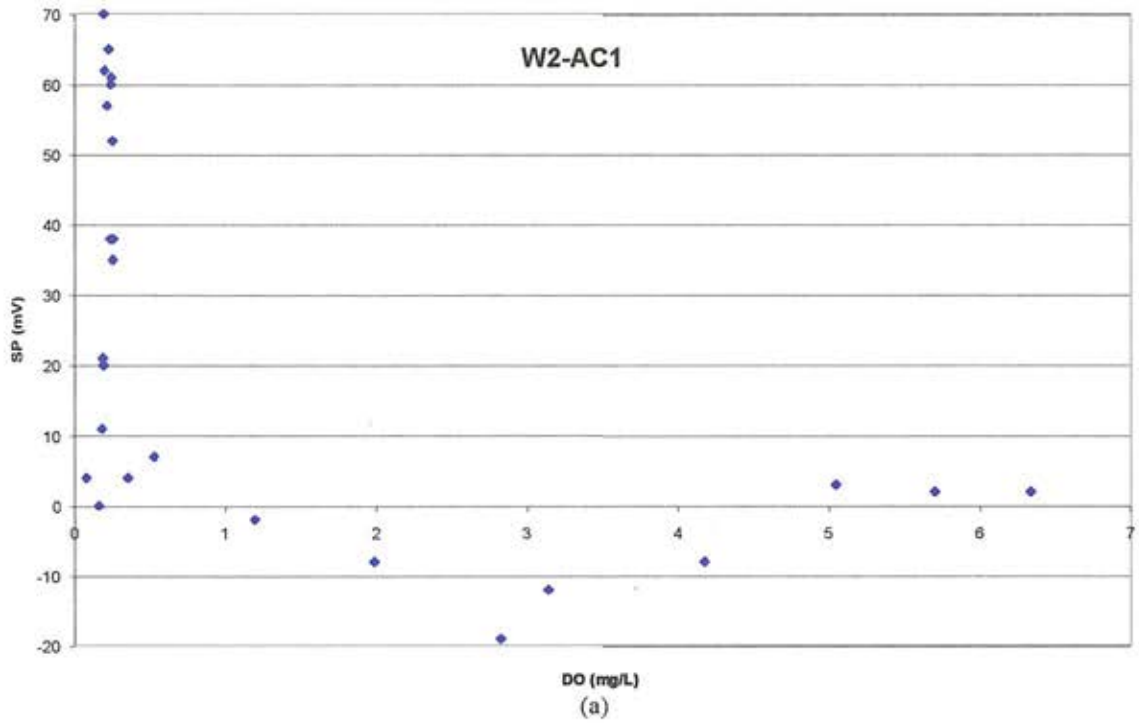


Figure 5-4. Plot of DO Versus SP for W2-AC1 & A3-TS5. Notice that both lines show a distinct nonlinear correlation between SP and DO when DO is below ~2 mg/L.

1971; Davis, 1973) for lines W2-AC1 and A3-TS5 also revealed a negative correlation between DO and SP. The Spearman rank correlation analysis ranked both the SP and DO data according to magnitude. The ranks were then tested to see if there was a correlation between the two data sets. The Spearman test yielded a coefficient that can be converted into a confidence level. The Spearman rank correlation coefficient for W2-AC1 was -0.55; AC3-TS5 was -0.90. Both coefficients were significant at the 99% confidence level. This test demonstrated that SP and DO are directly related to the subsurface phenomenon of the biodegradation of a contaminant plume.

CHAPTER 6

CONCLUSIONS

A. Summary and Implications

I conclude that a biogenetic redox plume can be mapped from the surface using SP when all other possible sources of SP have been accounted for. Choosing a field area with essentially no other sources of SP, except redox potentials associated with a contaminant plume, facilitated mapping the plume using SP.

To compare SP and redox results, I initially tried to directly measure the Eh from wells at the field site. I needed to use a surrogate parameter because direct measurements of Eh proved to be irreproducible. I concluded that DO was an appropriate surrogate parameter for Eh because contrasting DO conditions mimicked contrasting redox conditions. The contoured map of DO revealed anaerobic and aerobic zones corresponding to reducing and oxidizing redox conditions, respectively. Knapp and Thompson (1998) concluded that the anaerobic zone was created by the biological reduction of tomato waste by aerobic microbes based on DOC values and direct measurements of microbial populations from wells in the

field area. Repeated measurements of DO revealed that the plume of reduction has remained stable through time.

Background geophysical investigations at the Oyster site proved that the subsurface was electrically homogeneous. An electrically homogeneous subsurface was important because it allowed me to rule out other possible sources of SP besides redox reactions. A magnetic survey showed that the subsurface was devoid of buried ferrous material that could warp equipotentials or act as an undesirable source of redox. The resistivity survey showed that the subsurface possessed similar electrical properties throughout the field area. The GPR confirmed that two formations, with differing sedimentary structures, were present in the study area.

Data from two SP surveys taken at the site showed that two zones of differing voltages corresponded to the anaerobic and aerobic zones. There was strong negative correlation between SP and DO when the DO was below ~2 mg/L; above ~2 mg/L the SP remained fairly constant. Using a nonparametric statistical analysis (Spearman rank correlation analysis), I concluded that a negative correlation between the DO and SP existed with 99% certainty.

Bioremediation of contaminated sites has shown a lot of promise in the last decade as being a cheap and effective form of remediation. Using SP to remotely and continuously monitor bioremediation could reduce the need for monitoring wells and chemical analysis at contaminated sites. Preliminary SP characterization of a contaminated site could also facilitate the design of a monitoring well field. SP anomalies created by redox zonation support the validity of Corry's (1985) model. By furthering our understanding of the processes that create SP's, we can use SP monitoring to better our understanding of subsurface geochemistry.

B. Suggestions for Future Work

The existing well array at the field site was not designed for my study. A well array covering the entire area would better map the redox conditions throughout the field area. Additional wells around the redox boundary would also help resolve the boundary between the oxidizing zone and reducing zone.

Installation of a permanent SP monitoring system would be ideal for monitoring temporal fluctuations throughout the field area. An in-place monitoring system could also map the plume shape through time. To verify my study, a

similar study should also be conducted down-strike, away from the trenches, to show that there is no other SP source besides the redox plume. Laboratory analysis of which redox couples most influence SP could help explain the range in SP voltages over areas of biodegradation. Also, a down-hole SP survey in wells at the field area would show if the SP varies with depth. The SP method for mapping zones of reduction would be significantly refined if these future works were carried out.

REFERENCES CITED

- Belitz, K., and Burger, R. L., 1997, Measurement of Anisotropic Hydraulic Conductivity in Unconsolidated Sands; A Case Study from a Shoreface Deposit, Oyster, Virginia: *Water Resources Research*, v. 33, no. 6, pp. 1515-1522.
- Breiner, S., 1973, *Applications Manual for Portable Magnetometers*: Sunnydale, California, Geometrics, p. 43
- Bolster, C. H., Herman J. S., Hornberger, G. M., and Mills, A. L., 1999, Spatial Distribution of Deposited Bacteria Following Miscible Displacement Experiments in Intact Cores: *Water Resources Research*, v. 35, no. 6, ppb. 1797-1807.
- Chang, R., 1996, *Essential Chemistry*: McGraw-Hill, pp. 719.
- Christensen, T. H., Kjeldsen, P., Albrechtsen, H. J., Heron, G, Nielsen, P. H., Bjerg, P. L., and Holm, P. E., 1994, Attenuation of Landfill Leachate Pollutants in Aquifers: *Critical Reviews in Environmental Science and Technology*, v. 24, no. 2, pp. 119-202.
- Conover, W. J., 1971, *Practical Nonparametric Statistics*: John Wiley & Sons, Inc., p. 406.
- Corry, C. E., 1985, Spontaneous Polarization Associated with Porphyry Sulfide Mineralization: *Geophysics*, v. 50, no. 6, pp. 1020-1034.
- Corry, C. E., Madden, T., and Perry, J., 1996, Monitoring Leakage from Underground Storage Tanks Using Spontaneous Polarization (SP) Method: *Society of Exploration Geophysicists Annual Meeting Expanded Technical Program Abstracts with Biographies*, v. 66, pp. 932-935.
- Corwin, R. F., 1984, *Self-Potential Field Procedure and Data Reduction*: Unpublished Field Manual.

- Corwin, R. F., 1991, The Self-Potential Method for Environmental and Engineering Applications: Investigations in Geophysics, v. 5, pp. 127-145.
- Davis, J. C., 1973, Statistics and Data Analysis in Geology: John Wiley & Sons, Inc., pp. 98-99.
- Engesgaard, P., and Kipp, K. L., A Geochemical Transport Model for Redox-Controlled Movement of Mineral Fronts in Groundwater Flow Systems; A Case of Nitrate Removal by Oxidation of Pyrite: Water Resources Research, v. 28, no. 10, pp. 2829-2843.
- Ernstson, K., and Scherer, U. H., 1986, Self-Potential Variations with Time and Their Relation to Hydrogeologic and Meteorological Parameters: Geophysics, v. 51, no. 10, pp. 1967-1977.
- Fetter, C. W., 1993, Contaminant Geology: Upper Saddle River, New Jersey, Prentice-Hall, Inc., p. 458.
- Haq, B. U., Hardenbol, J., and Vail, P. R., 1988, Mesozoic and Cenozoic Chronostratigraphy and Cycles of Sea-Level Change: Society of Economic Paleontologists and Mineralogists Special Publication, no. 42, pp. 71-95.
- Knapp, E., and Thompson, A., 1998, Groundwater Contamination and Metal-Oxide Minerals in a Coastal Plain Sandy Aquifer: Virginia Journal of Science, v. 49, no. 2, p. 86.
- Kosanke, B. J., 1980, Aerial Radiometric and Magnetic Survey Map of Norfolk/Eastville Virginia: U.S. Geological Survey, scale 1:250000, 2 sheets.
- Lindberg, R. D., and Runnells, D. D., 1984, Groundwater Redox Reactions: An Analysis of Equilibrium State Applied to Eh Measurements and Geochemical Modeling: Science, v. 225, no.4665, pp. 925-927.
- Loke, M. H., and Barker, R. D., 1996, Rapid Least-squares Inversion of Apparent Resistivity Pseudosections by a Quasi-Newton Method: Geophysical Prospecting, vol.44, pp. 131-152.

- Mills, A. L., and Powelson, D. K., 1998, Water Saturation and Surfactant Effects on Bacterial Transport in Sand Columns: *Soil Science*, v. 163, no. 9, pp. 694-704.
- Mixon, R. B., 1985, Stratigraphic and Geomorphic Framework of Uppermost Cenozoic Deposits in the Southern Delmarva Peninsula, Virginia and Maryland: U.S. Geological Survey Professional Paper 1067, pp. 53.
- Mixon, R. B., 1985, Generalized Geologic Map and Cross Sections of the Southern Delmarva Peninsula, Virginia and Maryland: U.S. Geological Survey, scale 1:250000, 2 sheets.
- Oertel, G. F., 1987, Barrier Island Processes and Environments on the Eastern Shore of Virginia: *Marine Geology*, v. 69, pp. 179-188.
- Reynolds, J. M., 1997, *An Introduction to Applied and Environmental Geophysics: West Sussex, England*, John Wiley & Sons Ltd., p. 796.
- Sato, M., and Mooney, H. M., 1960, The Electrochemical Mechanism of Sulfide Self-Potentials: *Geophysics*, v. 25, pp. 226-249.
- Telford W. M., Geldart L. P., and Sheriff, R. E., 1990, *Applied Geophysics: New York, New York*, Cambridge University Press, 2nd ed., p. 770.